1

A Journey from Molecular Phthalocyanines to Polymeric Materials

1.1 Introduction

Throughout the progress of human civilization, innovations in materials always promote the breakthrough of science and technology, resulting in the great promotion of productivity and the tremendous development of human society. In other words, materials are the foundation of civilization development. A variety of materials covering stone, copper, bronze, iron, inorganic silicon, and organic molecular and polymeric species successively innovate tools, methods, and even ideology that have not only survived human beings from nature's challenges but also endowed them the comprehensive capability to resist and use nature [1]. Thus far, new materials design and preparation still highly contribute to the technological innovations for targeted applications. This could guarantee plenty of energy resources' supply, health and longevity of humankind, and sustainability of economy, ecology, and civilization [1]. In this regard, chemistry has always aimed to produce new matters and to understand the structures and functions behind these matters for predicting desired functions [2]. In classical chemistry, chemists intend to prepare pure inorganic and molecular compounds by means of the broken and formation of strong covalent bonds into/from atoms for understanding nature from atom and molecular perspectives [2]. These well-defined materials are different from those of the most important biological systems with imprecise structures assembled from non-covalent interactions. It is worth noting that the dynamic nature of biological architectures originated from weak interactions, which plays an important role in the complicated physiological activity of living systems. In this context, the enormous difference in structures together with properties and functions between the artificial and natural chemical compounds arouse the renovations of materials synthesis approaches through the mode of atom by atom and/or molecule by molecule.

Supramolecular chemistry is also well known as "chemistry beyond the molecule." [2] It has been established since 1987 as a result of the Nobel Prize in Chemistry awarded to Donald J. Cram, Jean-Marie Lehn, and Charles J. Pedersen "*for their development and use of molecules with structure-specific interactions of high selectivity*." [2] Since then, supramolecular chemistry has flourished following its application in the organization of chemical systems to mimic biological processes, bridging biological and materials science. However, the initial study in the field

Phthalocyanine-Based Functional Polymeric Materials: Design, Synthesis, and Applications,
First Edition. Jianzhuang Jiang, Hailong Wang, and Kang Wang.

of supramolecular chemistry focused on molecular recognition phenomena as early as and even before macrocyclic chemistry, crown ether chemistry, and host–guest chemistry has emerged to enrich the concepts and perspectives in the field of supramolecular chemistry [3]. In the recent 20 years, the intrinsically dynamic characteristic of supramolecular chemistry has gradually attracted attention, expanding its scope to the dynamic covalent chemistry and dissipative self-assembly processes [4]. In the future, there must be still many directions that will be discovered from comprehensive researches.

Today, the development of materials design and preparation still continues to focus on their eternal theme applications for enabling sustainable global resources and environments as well as human health [5]. Simultaneously, there are many efforts dedicated to molecular engineering by using atoms and molecules to assemble polymeric materials toward the targeted properties and functions, providing a bottom-up approach to prepare polymeric structures through various interactions. Molecular engineering of the interactions and spatial arrangement of rationally selected molecular modules holds promise for fine-tuning the functions of molecule-based materials. Instead of the sole discussion of strong chemical interactions between atoms in molecules, the advancement of polymeric materials requires understanding the relationships between the functions and the complicated factors that are involved in the polymeric structural materials beyond molecular components. From atomic and molecular perspectives, the well-defined polymeric assemblies in crystalline states are very helpful in precisely correlating the structure-function relationships behind the increased complexity of these materials architecture because their well-defined chemical structures enable the elucidation of their electronic structures. In this direction, metal–organic frameworks (MOFs, since 1999) [6], covalent organic frameworks (COFs, 2005) [7], metal-organic cages (MOCs, 1995) [8], and various porous organic crystals including porous organic cages (POCs, 2009) [9] and hydrogen-bonded organic frameworks (HOFs, 1994) [10] have been established, which enrich the "chemistry of the framework." Their constituent components with variable geometries, sizes, and functions play an important role in attaining designable structural topology, adjustable homogeneous porosity, and tunable functionalities for these materials, enabling a lot of diverse applications in the field of gas storage, separation, catalysis, and energy storage and conversion. In particular, the open frameworks usually have permanent nanometer-sized voids that ensure molecular recognition, chemical storage, stereoselective conversion of molecules, and powerful support to encapsulate various nanomaterials of metals, metal oxides, semiconductors, and complexes. As a result, these frameworks have always attracted the wide and intense attention of researchers from chemistry and materials fields.

Phthalocyanines (Pcs) are very important blue or green commercial pigments used in inks, as a dyestuff for textiles, and as a colorant for metals and plastics due to the intense Q-bands at 620–700 nm, and their history is dated from 1928 [11–13]. The characterizations of their structures were first introduced in 1934 [14–17]. X-ray diffraction analyses performed by Robertson clearly reveal that the planar macrocyclic molecular structure of Pc contains the four isoindole units connected by four

aza-bridges [18–20], possessing an 18-electron aromatic cloud delocalized over 16 alternated carbon and nitrogen atoms surrounding the N_4 cavity. Such a macrocyclic structure for artificial Pcs is very similar to that of the naturally occurring porphyrins (Pors), exhibiting strong electronic absorption ability in the visible light region and an excellent photosensitive property to fast transfer energy and/or electron to its acceptor counterparts [21–23]. Therefore, Pcs are also widely investigated in artificial photosynthetic systems and nanomedicines due to their huge molar absorption coefficients in the red near-infrared range, fluorescence, phosphorescence, singlet oxygen generation quantum yields, and adjustable photochemical properties from molecular perspective [22–27]. For example, Pcs have been used as important photosensitizers for fluorescence imaging and photodynamic therapy [26, 27]. Different from Pors, Pcs also have significant thermal and chemical stability due to the special conjugation structures, supporting the harsh sublimation process and intense electromagnetic radiations. As a result, the well-defined structure of metal-free Pc (H_2Pc) as the first organic compound was resolved using single-crystal X-ray diffraction (SCXRD) technology [28].

The remarkable versatility of molecular Pcs could be further improved by replacing the central two hydrogen atoms in the N_4 cavity with more than 70 metals as well as by introducing the functional substituents on the non-peripheral (α) and peripheral (β) positions and even the axial positions of the macrocycle (Figure 1.1). In particular, the large homo- and heterometallic ions (e.g. rare earths [REs], actinides, and group 4 transition metals) enable the complexation with macrocycles to form sandwich-type complexes in the form of double-, triple-, quadruple-, quintuple-, and sextuple-decker structures. The intramolecular π-π interactions and the metal attributes make these compounds interesting properties and good device candidates in the field of field-effect transistors, molecular magnets, information storage materials, and sensors. The intrinsic monomolecular and supramolecular characteristics of Pcs therefore are not only fine-tuned but also greatly innovated

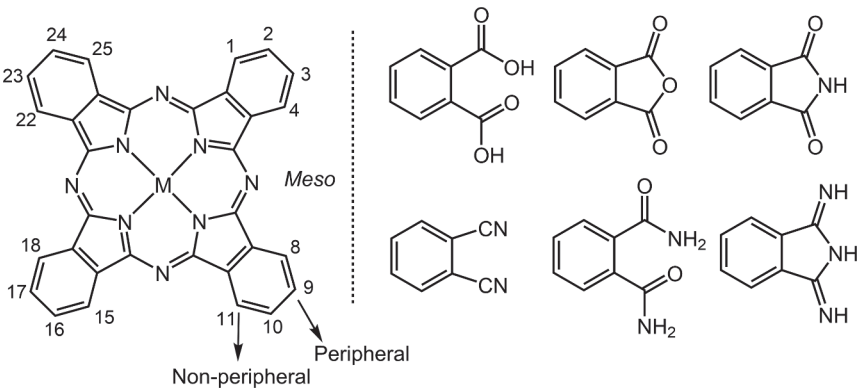

Figure 1.1 (a) Phthalocyanine core and various precursors (M = metal and 2H. 1, 4, 8, 11, 15, 18, 22, 25 and 2, 3, 9, 10, 16, 17, 23, 24 sites are non-peripheral (α) and peripheral (β) positions, respectively. The substituents are omitted for clarity). (b) Partial phthalocyanine precursors.

due to the macrocycle metalation and modification. Thus far, Pcs have been well developed and widely explored in the field of fundamental research and industrial and technological areas. They have been used as active components to fabricate semiconductors [29], chemo-sensors [30, 31], electrochromic displays [32, 33], information storage devices [34, 35], liquid crystals [36, 37], photovoltaic cells [38, 39], catalysts [40, 41], and nonlinear optics and optical limiting materials [42–44]. In addition to possessing diverse chemistry, molecular Pcs serve as functional building blocks (also named synthons) to assemble multicomponent and even polymeric systems [40–42, 45]. The diversity of linkages and modules provides the abundant assembly chemistry of Pcs macrocycles, further broadening their applicability and strengthening their stability toward practical use. It is worth noting that the spatial arrangement of Pcs macrocycles, module types, and connection modes is crucial for the positive expression of their functionalities and properties. The supramolecular and covalent organization guarantees the fine control of the spatial arrangement of Pcs building blocks and/or appropriately paired counterparts. The corresponding structure and property studies are of importance and compatible with each other from supramolecular and covalent polymer levels. Within this context, the porosity formed by the stacking Pcs macrocycles is able to take advantage of the substrate confinement, diffusion, and activation, enabling the formation of a kind of unique porous polymeric material.

In this chapter, we intend to summarize the preparation and applications of functional Pcs to provide a basic research background for the focused polymeric materials research in this book. Their basic synthetic methods ensure the preparation of powerful monomers for constructing polymeric materials through various reactions occurring on the active moieties. We also describe how the versatile chemistry makes the Pc materials evolve from monomers, oligomers, composites, supramolecular assemblies, dendrimers, to polymers. In addition, we focus on the most recent contributions in functional Pcs mainly since 2010, and the outstanding paradigms of Pc-based polymeric materials (MOFs and COFs) and applications (electrocatalysts, sensors, etc.) are also introduced. These diverse heterogeneous application studies at the molecular level accumulate enough knowledge to improve the functionalities of polymeric materials.

1.2 Monophthalocyanines

Molecular engineering is the main ideological system passing through the design and preparation of materials made up of discrete molecules for the targeted function, requiring precise understanding and thus tuning the structure–function relationships inherited in the molecule-based materials at the atomic/molecular level. A large number of factors that are involved in the assembly of molecular (microscopic) components to aggregated (macroscopic) solids increase the complexity in correlating the structure–function relationships of the latter complicated materials than those of their individual building blocks. These factors across a number of length scales, including the changed microscopic environments of molecular modules in

materials, the connection modes, spatial arrangement, aggregated degrees, materials defects, sizes and morphologies of materials, and working environments, etc. These principles in molecular engineering are certainly suitable for the development of Pc-based polymeric materials. To date, Pcs have been demonstrated as versatile molecular modules in the assembly of polymeric materials through appropriate organization modes and linkages [46–48]. Many efforts in engineering the properties of these materials depend on bottom-up approaches based on molecular Pcs for fabricating composite polymeric structures toward rational optimization of their practical and multifaceted functions [49–53]. Within this context, the design and preparation of molecular Pcs is of prime importance, ensuring the successful assembly of these macrocyclic building blocks into the desired spatial arrangements for obtaining optimal optoelectronic properties.

Phthalonitriles, phthalic anhydride, phthalimide, and 1,3-diiminoisoindoles are common starting materials for the preparation of molecular Pcs for constructing supramolecular and covalent-bonded composites and polymeric compounds (Figure 1.1). The cyclization arrangement of aza-connected four isoindole units at their 1,3-positions in a reasonable yield usually occurs with the help of metal ion template (such as metal, salt, alkoxide, or metal salt/organic amine) reaction under a solution upon reflux in C3–C8 alcohols at 100–200 °C or in 2-(*N*,*N*-dimethylamino [DMF]) ethanol at 135 °C [54]. For solution reactions, the non-nucleophilic base catalysts such as 1,8-diazabicyclo[5.4.0]undec-7-ene (DBU) are necessarily employed for the formation of Pcs. For example, the preparation of metallic macrocycles (NiPcs) has been demonstrated from phthalonitrile with the help of divalent nickel salt in a solution of amine (e.g. quinoline, DMF, ethanol, DBU, and urea), hydroquinone, and alkali and additional activation by microwave or ultraviolet (UV) irradiation [55]. In good contrast, solid-state reactions have emerged as a sustainable and environmentally friendly approach to obtain Pc chemicals due to the avoidance of solvent use. These synthetic routes have been previously summarized in several reviews and books, detailing various smart methods of symmetric and asymmetric Pc molecules [12]. In recent years, mechanochemical preparation has been studied to couple with solid-state synthesis of Pcs for further promoting the production yield and the direct synthesis of composite materials for diverse applications [56]. In this section, the contributions in the design and synthesis of Pc compounds with active sites for aggregation and polymerization, which could be extended from molecules, oligomers to diverse composites and assemblies, have been selectively introduced for the after-mentioned research. Actually, the chemical alternations on the four benzene rings at the α and β positions of Pcs are basically achieved using various organic synthetic methods (Figure 1.1). The incorporation of active groups mainly occurs on β positions of Pc scaffolds. Four or eight functional groups including amino groups, carboxylic groups, hydroxyl groups, cyano groups, iodine atoms, fluorine atoms, and alkynyl groups on macrocyclic rings are helpful in the polymerization of discrete molecular modules into various photoactive and/or electroactive coordinate- and covalent-bonded assemblies as well as multicomponent systems. In the following section, we present the preparation of four- and eight-substituted Pcs to introduce these building blocks with four and eight active atoms/groups, respectively.

1.2.1 Tetra-Substituted Monophthalocyanines

Among the above-mentioned active groups, the nature of amino, carboxyl, hydroxyl, and cyano species of Pcs permits both coordination and covalent polymerization. In contrast, iodine atoms, fluorine atoms, and alkynyl groups allow only covalent expansion of Pc macrocycles. Pc macrocycles attached by four amino groups attract great interest due to the simple preparation process of their nitro-substituted macrocycle precursor. All 4-nitrophthalonitrile, 4-nitrophthalic anhydride, 4-nitrophthaloimide, and 4-nitrophthalic acids as starting materials have been converted into macrocyclic Pcs present in various metal salts according to the reported literature [57–59]. For example, the reaction of metal salts, 4-nitrophthalic acid, ammonium chloride, ammonium molybdate, and urea in nitrobenzene at 185 °C led to the generation of metallic tetranitrophthalocyanine isomers, which was further reduced by Na_2S to obtain the corresponding tetraaminophthalocyanine with yield up to 90%. Such preparation method was suggested to obtain metallic tetraaminophthalocyanine-containing metals with ionic radii of about 0.8 Å, including copper, cobalt, nickel, zinc, iron, platinum, aluminum, and vanadium (Figure 1.2).

In addition, the preparation of Pcs with active iodine substituents is also of high interest because the functional group allows the chemical modification to provide new building blocks for polymeric structures through metal-catalyzed reactions. The high diversity of the functionalization via arylhalides precursors has been demonstrated as indicated by various organic synthetic materials. Herein, zinc tetraiodophthalocyanine is taken as a representative, which is prepared using a solid reaction of 4-iodo-phthalonitriles with metal salt at 220–250 °C [60]. Then, vinylsulfo groups were attached to on the isoindole rings of zinc tetraiodophthalocyanine through its Heck reaction with sodium vinylsulfonate with the help of Pd(II)acetate catalyst. Such a strategy allows the fabrication of not only acetylene- or vinyl-containing Pcs but also a wide range of functional group-attached scaffolds. In contrast to the chemical synthesis from tetraiodophthalocyanine as precursors, there is an example for the direct synthesis of functional Pc building blocks using functional dicyanide. The terpyridine precursor (4′-(4,5-dibromo-2-methylphenyl)-2,2′:6′,2″-teryridine) was provided based on the Kröhnke method using 4,5-dibromo-2-methylbenzaldehyde to react with 2-acetylpyridine and then 1-(2-pyridylcarbonylmethyl)pyridinium iodide with the

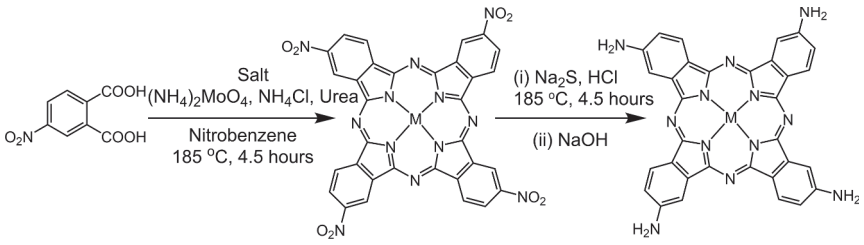

Figure 1.2 Preparation of metallic tetraaminophthalocyanine building block.

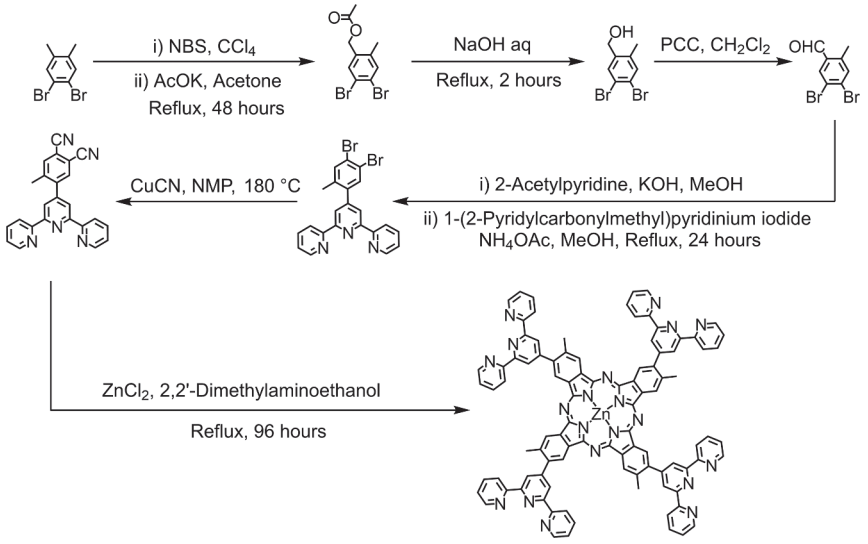

Figure 1.3 A Rosenmund-von Braun reaction yields dicyanides, which are converted into the corresponding ZnPc by refluxing in 2-(dimethylamino)ethanol in the presence of $ZnCl_2$.

assistance of ammonium acetate [61]. In the following step, a Rosenmund-von Braun reaction of 4′-(4,5-dibromo-2-methylphenyl)-2,2′:6′,2″-teryridine with CuCN gave the dicyanide compound (4′-(4,5-dicyano-2-methylphenyl)-2,2′:6′,2″-teryridine), which proceeded the cyclization to provide the corresponding zinc Pc bearing four terpyridine units by refluxing in 2-(dimethylamino)ethanol containing $ZnCl_2$ (Figure 1.3). The terpyridyl-containing Pc and another mono-terpyridine ligand were used to assemble multicomponent systems composed of Pcs and bis(terpyridyl) metal complexes through a stepwise synthetic procedure.

Carboxyl and sulfo groups are active sites for supramolecular and covalent composites and polymers. The preparation of carboxyl-attached Pcs is taken as an example. For the Pcs with carboxyl groups attached to on the peripheral positions, they are prepared by the reaction of trimellitic anhydride, urea, and metal salts in nitrobenzene with the help of a catalyst followed by the hydrolysis reaction [62]. In addition, the substitution of 4-nitrophthalonitrile, 4,5-dichlorophthalonitrile, or 3,4,5,6-tetrachlorophthalonithrile with ethyl 4-hydroxy-3-methoxybenzoate generates the corresponding phthalonitrile derivatives (Figure 1.4). The carboxyl-containing Pcs have been prepared by the above-mentioned conventional methods. The functional substituents in the isoindole ring of Pcs could enhance their solubility due to the steric strain inhibiting the π-π interaction of the macrocycle [63, 64].

1.2.2 Octa-Substituted Monophthalocyanines

Octa-substituted Pc building blocks are those molecules with eight substituents including amino, carboxyl, hydroxyl, fluorine, and cyano species located on the

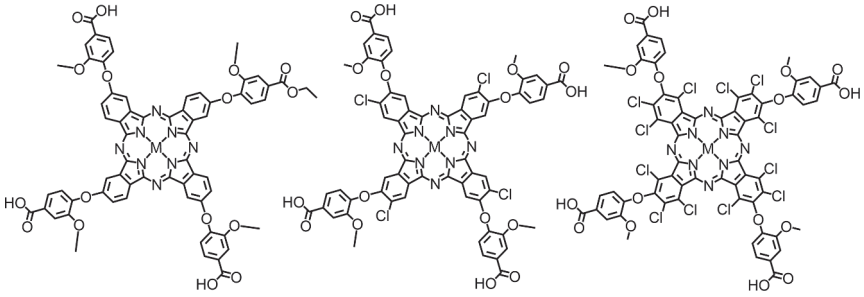

Figure 1.4 Structures of carboxyl-bearing phthalocyanines.

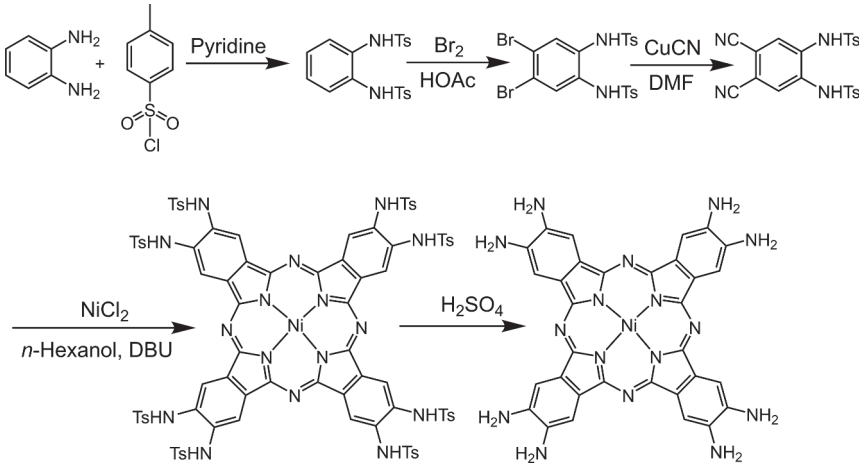

Figure 1.5 Preparation of metallic octaaminophthalocyanine building block.

peripheral positions of the macrocycle. Generally, these monomeric Pcs are prepared from their corresponding phthalonitriles followed by the necessary deprotection and metalation. For 2,3,9,10,16,17,23,24-octaaminophthalocyanine, its starting material, *o*-phenylenediamine, was first tosylated with tosyl chloride, brominated by liquid Br_2, and then reacted with CuCN to generate 4,5-dicyano-*N*,*N*′-ditosyl-*o*-phenylenediamine. Metal-free 2,3,9,10,16,17,23,24-octaaminophthalocyanine was achieved through protonation of the dilithium Pc intermediate prepared by heating *n*-pentanol containing lithium and dicyanide compounds followed by a proton–lithium exchange. In contrast, the cyclotetramerization reaction of 4,5-dicyano-*N*,*N*′-ditosyl-*o*-phenylenediamine in the presence of the metal salt and DBU in refluxing *n*-hexanol led to metallic species [65]. 2,3,9,10,16,17,23,24-Octaaminophthalocyanine nickel(II) was prepared by the deprotection in the presence of H_2SO_4 (Figure 1.5) [66]. Obviously, most phthalonitriles as Pcs' precursors are prepared by the energy- and time-consuming synthesis process, including the introduction of a protective group, bromination, and cyanidation. The necessary deprotection is required for those Pc molecules with active sites for the next assembly. As a result, the improvement of the synthesis route for symmetric Pcs is

of significance for the development of polymeric materials. It is worth noting that the axial ligand coordination of Pcs provides another possible approach to construct polymeric materials. In this direction, silicon or ruthenium Pcs are also modules for the introduction of axial ligands to assemble oligomers and dendrimers. In addition, some molecular Pcs with four different isoindole rings (denoted as asymmetric species) are also useful building blocks for the construction of oligomers and polymers, which are prepared by mixed phthalonitriles, usually exhibiting a low yield after tedious separation.

1.3 Phthalocyanine-Based Oligomers

1.3.1 Sandwich-Type Phthalocyanine-Based Complexes

Sandwich-type tetrapyrrole compounds are classified as homoleptic and heteroleptic species. Homoleptic sandwich-type compounds are made up of the same phthalocyaninato or porphyrinato ligands (Figure 1.6). In contrast, heteroleptic compounds constitute two different tetrapyrrole ligands, which belong to the same subclass of species. When the sandwich-type compounds involve two kinds

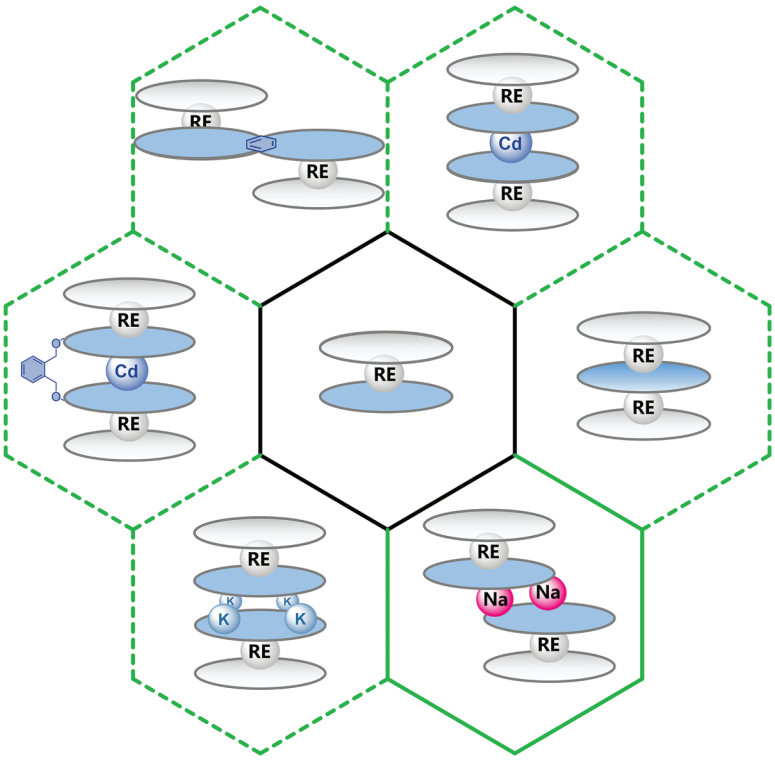

Figure 1.6 Schematic diagram of sandwich-type phthalocyanine-based complexes. Source: Reproduced from Ref. [67] / with permission of John Wiley & Sons.

of tetrapyrroles with one as Por, they are denoted as mixed sandwich-type compounds [68]. The discovery of homogeneous bisphthalocyaninate, $Sn(Pc)_2$, in a double-decker structure dates from 1936 [69]. This compound has been constructed from the reaction of $(Pc)SnCl_2$ and $Na_2(Pc)$. In 1965, the first RE Pcs were discovered by Kirin and Moskalev [70]. The electrochromic behavior of bisphthalocyanine RE compound $RE(Pc)_2$ was demonstrated in 1979 due to the presence of three ligand-based redox transformations including anionic $[(Pc^{2-})M^{3+}(Pc^{2-})]^-$, neutral $[(Pc^{2-})M^{3+}(Pc^{\bullet-})]^0$, and cationic $[(Pc^{\bullet-})M^{3+}(Pc^{\bullet-})]^+$ forms. The difference in spectrum and the presence of radical of three forms in different colors attracted intense researchers' interest. The definite molecular structure of double-decker neodymium bisphthalocyaninate, $Nd(Pc)_2$, was revealed by SCXRD technology in 1980 [71].

The big ionic radii and the high coordination numbers of RE ions ensure the formation of not only the double-decker but also the triple-decker metal Pc compounds under optimal reaction conditions. The study of homogeneous tris(phthalocyaninato) RE metal compound was started based on the landmark compound $[Y_2(Pc)_3]$ in 1986 [72]. In these stacking sandwich-type complexes, the inter-macrocycle π-π interactions make them unique optical and electrochemical properties, and the eight-coordination geometry of paramagnetic RE metals further expands their applications to the active fields of molecular magnetism and spintronics [73, 74]. Actually, the investigations of the reaction conditions for double- and triple-decker RE compounds have been intensely performed, giving birth to several useful protocols. Generally, the template tetracyclization of phthalonitriles and RE salts mainly yields double-deckers in high boiling point alcohols with the help of DBU under low temperatures [75]. On the contrary, the reactions between as-prepared Pcs and metal salts refluxed in high boiling point solvents prefer fabricating the mixture of double- and triple-decker complexes, and high temperatures and long reaction times are helpful for the formation of triple-decker species. Since 2010, the investigation of the construction, characterization, and properties of multiple-decker heterometallic (RE/cadmium) complexes made up of four, five, and six tetrapyrrole macrocycles has initiated a new family of sandwich-type compounds. [76] The double-decker RE compounds have been used as building blocks to react with cadmium and monomeric Pcs to generate multiple-decker compounds in 1,2,4-trichlorobenzene (TCB) [77]. It is worth noting that such double-deckers were able to directly construct sandwich-type quadruple-decker Pc-based compounds in solid-phase reactions at high temperatures [78]. Among these multiple-decker compounds, the electronic coupling between the RE centers and molar absorption coefficients is decreased following the increased number of Pcs, discovering the intramolecular electronic coupling of macrocycles relied on the RE ion size and the super-distance metal–metal interactions. [79, 80]

The study of heteroleptic sandwich compounds had been started in the early 1990s [81]. The preparation of heteroleptic double-deckers M(Pc′)(Pc′′) (Pc′ and Pc′′ represent different Pcs) with different Pcs has been performed with the one-pot reaction of 4-propoxyphthalonitrile, 4-*tert*-butylphthalonitrile, and lutetium acetate at 290 °C, followed by the tedious column chromatography purification due to the mixed products with similar molecular polarity. Thus far,

the reported heterogeneous double-deckers M(Pc′)(Pc′′) are usually prepared by the reaction of the half-sandwich Pc compounds and various substituted Pcs. Alternatively, they are obtained by the reaction of half-sandwich Pcs and phthalonitriles in the presence of DBU. The production yield for these heteroleptic species is usually low due to the generation of homoleptic side products. Triple-deckers in the form of $(Pc')M^1(Pc'')M^2(Pc')$ and $(Pc')M^1(Pc')M^2(Pc'')$ (M^1 and M^2 could be either the same metal ions or the different metals) could be prepared by the reaction of double-decker compounds, monophthalocyanine, and RE salt or double-decker compounds and half-sandwich-type compounds in high boiling point solvents. Heteroleptic quadruple-deckers were fabricated by the complexation of heteroleptic double-deckers or two different double-deckers with cadmium ion, where the preferred localization of cadmium is between the two electron-rich Pcs. It is worth noting that there is an interesting example composed of cadmium metalation of clamshell-type dimeric Pcs to form sandwich-type quadruple-decker complexes [82]. In addition, the fused Pcs connect double-decker and triple-decker subunits together to afford heteroleptic binuclear and tetranuclear RE sandwich-type compounds through the one-pot and stepwise methods. At the end of this paragraph, the heteroleptic bis(phthalocyaninato) RE double-deckers are connected by alkali metal ions (such as Na^+ and K^+ coordination with non-peripheral octaalkoxy-substituted and peripheral crown-substituted Pcs) to generate supramolecular pseudo-quadruple-decker compounds (Figure 1.7) [67, 83, 84]. Heterometallic multiple-decker complexes with up to six decks have been prepared by the homoleptic/heteroleptic double-deckers to react with cadmium ions and monophthalocyanine in refluxed TCB [85].

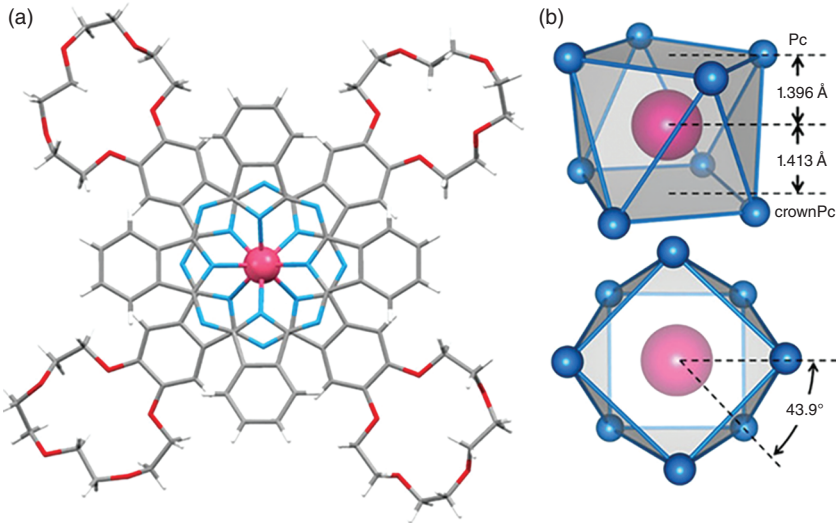

Figure 1.7 (a) Crystal structure of terbium(III)-phthalocyaninato double-decker complexes with crown moieties and square antiprism (SAP) coordination environment (pink: Tb, gray: C, red: O, blue: N, white: H). Source: Reproduced from Ref. [83] / with permission of John Wiley & Sons.

Mixed Pc-based compounds in the form of triple-decker structure involving phthalocyaninato and porphyrinato ligands were discovered in 1986 [86], which are provided from a refluxed TCB solution of dilithium phthalocyaninate and mono(porphyrinato)-lanthanide generated from meso-tetrakis(4-methoxyphenyl) Por and $RE(acac)_3$ (RE = Nd, Eu, Gd). These triple-decker compounds were also prepared in modest yields through unseparated RE monoporphyrinates reacting with double-decker $M(Pc)_2$ in refluxing TCB. The first triple-decker species, [(Tpp)Ce(Pc)Gd(Oep)], Oep = octaethylporphyrin dianion, composed of both different metals and macrocycles, was reported in 1996, and its molecular structure has been clearly disclosed by SCXRD determination [87]. In contrast, the mixed phthalocyaninato and porphyrinato double-decker sandwich-type compounds were obtained later. Their preparation, crystal structures, and spectroscopic properties have been systematically studied with the representative of the neutral [(TPP)RE(Pc)] (TPP and Pc = dianions of tetraphenylporphyrin and Pc, respectively; RE = La, Pr, Nd, Eu, Gd, Er, Lu, and Y in trivalent redox state), which were fabricated by the reaction of dilithium Pc and metal acetylacetonate $M(acac)_3$ and then tetraphenylporphyrin [88]. Similar to the neutral double-decker Pc RE compounds, they have the characteristic spectroscopic properties of a one-electron-oxidized radical-containing Pc ring ($Pc^{\bullet-}$). As a result, these radical-containing Pc rings can be transformed to $[(TPP^{2-})RE(Pc^{2-})]^{-}$ and di-π-radical $[(TPP^{\bullet-})RE(Pc^{\bullet-})]^{+}$. These different redox states of double-deckers also influence the behaviors of single-molecule magnets [89]. In addition, the preparation of mixed (phthalocyaninato)(porphyrinato) double-deckers was based on the template reaction of the half-sandwich porphyrinato RE compound with phthalonitrile compounds. Since 2012, the mixed (phthalocyaninato)(porphyrinato) compounds have attracted new interests due to the excellent crystallinity and D_{4d} coordination geometry around paramagnetic lanthanide ions for single molecular magnets [90]. Thus far, there are three forms of mixed triple-deckers, including $[(Por')M^1(Pc')M^2(Por')]$, $[(Por')M^1(Pc')M^2(Pc'')]$, and $[(Pc')M^1(Por)M^2(Pc')]$ [91]. Notably, a mixed (phthalocyaninato)(porphyrinato) quadruple-decker RE-Cd compound was derived from the one-pot reaction of mixed double-deckers and homoleptic double-deckers in the presence of cadmium acetate in 2011 [92]. In addition to the homoleptic and heteroleptic Pc-based compounds and mixed (phthalocyaninato)(porphyrinato) metal complexes, there are few examples where the RE metals are sandwiched between the Pc and other macrocycles, such as corrole [93], *N*-confused Por [94], hemiporphyrazine [95], Salen [96, 97], and cyclen ligands [98]. In particular, mixed Pc and Salen metallic compounds have been built in the form of double-, triple-, and quadruple-decker structures.

1.3.2 μ-Oxo-Linked Phthalocyanine-Based Oligomers

μ-Oxo-linked oligomers were defined as those compounds with a metal center of Pc and/or other species bridged by a single μ-oxo atom to generate bi-, tri-, and oligonuclear macrocyclic compounds (Figure 1.8) [99]. SiPc species are one of the most well-known μ-oxo-linked Pc-based oligomers [100]. μ-Oxo-linked SiPc dimers

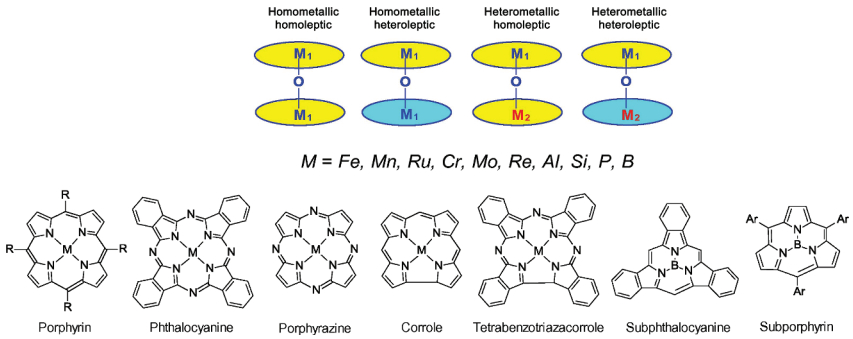

Figure 1.8 General structures of homo- and heterometallic complexes in homo- and heteroleptic ligand environment. Source: Reproduced from Ref. [99] / with permission of Elsevier.

are easily formed from a refluxing toluene solution of $SiPc(OH)_2$ in the presence of $CaCl_2$ [101]. In addition, various μ-oxo dimers of metallic Pcs of Al, Ti, Mn, Fe, and Cr metals have been reported [99]. For example, both μ-oxo diiron unsubstituted and substituted Pcs have been prepared. The first μ-oxo dimer with a bent Fe-O-Fe moiety is capable of being obtained from monomeric iron Pcs in organic solvents (DMF, dimethylacetamide [DMA], tetrahydrofuran, dioxane, and dimethyl sulfoxide [DMSO]) in air [102]. In contrast, the other kind of μ-oxo dimers with a linear Fe-O-Fe moiety has been prepared in either a mixed solution of 96% H_2SO_4 and 1-chloronaphthalene or 2-propaneamine. In addition, they are also fabricated using 96% H_2SO_4 and then precipitated with water. Since 1999, the catalytic properties of μ-oxo-linked iron Pc dimer have been demonstrated toward the oxidation of aromatic compounds to quinones [103], showing superior catalytic properties than the corresponding mononuclear counterparts due to the unique dimeric structure for the former system [99, 104]. Due to the technological development of gel permeation chromatography, μ-oxo SiPc trimers and tetramers have been successfully purified from the mixture prepared by the condensation products of $SiPc(OH)_2$. This series of μ-oxo SiPc oligomers has attracted much attention owing to the cofacial macrocyclic π-conjugation structures with an interplanar distance of 3.3 Å [105]. In addition to the μ-oxo homoleptic Pc oligomers, there are also heteroleptic Pc and other tetrapyrrole oligomers [106], as well as single μ-nitrido- and μ-carbido-linked dimers [107, 108]. Single μ-nitrido diiron Pcs are constructed from a boiling chloronaphthalene of monomeric iron Pcs or μ-oxo diiron Pcs reacting with NaN_3. These μ-nitrido diiron Pcs have been used for a series of difficult organic transformations, including oxidation of methane and benzene, transformation of aromatic C–F bonds, oxidative dechlorination, and formation of C–C bonds under clean and mild conditions.

1.3.3 Phthalocyanine-Based Supramolecular Oligomers

Organic synthesis and supramolecular chemistry bring a tight tap between molecular design and the study of Pcs' properties. In these directions, coordination interactions between metals and ligands have been widely used to

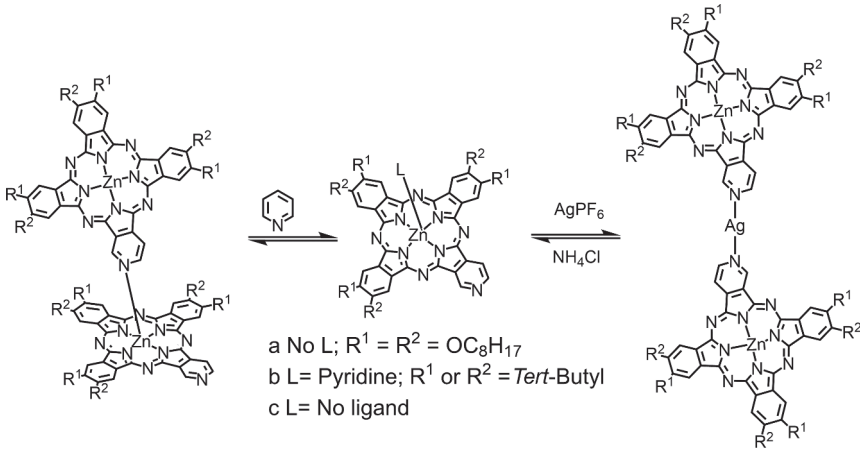

Figure 1.9 Zn(II) pyridino[3,4]tribenzoporphyrazine and two modes of self-assemblies. Source: Adapted from Refs. [3, 4].

prepare supramolecular materials. Thus, it is also an important toolkit to construct supramolecular oligomers and polymers based on Pcs. As early as in 1997, homogeneous Pc dimer was formed by metal–ligand interactions between Zn(II) hexaoctylpyridino[3,4]tribenzoporphyrazine derivative [109]. In this study, the metal-free macrocycle with a yield of 10% was prepared by the reaction of 3,4-dicyanopyridine with excess 3,6-dioctylphthalonitrile with the help of $C_5H_{11}OLi$. The asymmetric Pc monomer contains three isoindolic moieties and a pyridine (py) unit in refluxing pentanol, forming edge-to-face dimer through the complexation of the py moiety with zinc atom from another compound in the axial direction. In contrast, the replacement of zinc ion with nickel ion only leads to face-to-face aggregates. The similar coordination-bonded dimers composed of py unit-containing Pc compounds have been studied by other groups [110, 111] (Figure 1.9). These dimeric compounds have been explored using electronic absorption spectroscopy, fluorescence spectroscopy, magnetic circular dichroism spectroscopy, and time-resolved electron paramagnetic resonance spectroscopy.

Most of the Pc-based supramolecular structures based on coordination bonding interactions involve the Zn(II) and Ru(II) species. In 2005, hexa-*n*-butoxyimidazolylphthalocyaninato zinc compound was constructed through the condensation between 6-cyanodiiminoisoindoline and excessive 6,7-dibutoxydiiminoisoindoline with the assistance of $Zn(OAc)_2$ (Figure 1.10) [112]. Its cyan group is further reacted with *N*-methylethylenediamine to form an imidazolinyl substituent followed by oxidation of the imidazolinyl derivative with 5% Pt/C to form zinc hexa-*n*-butoxyimidazolylphthalocyanine. In addition, 2-(1-methyl-2-imidazolyl)-9(10),16(17),23(24)-tri-*tert*-butylphthalocyaninato zinc and 2-(1-methyl-2-imidazolyl)-9(10),16(17),23(24)-tri-*tert*-butylphthalocyaninato magnesium were prepared using the similar method. The self-association behaviors of these compounds have been checked by titrations in toluene using ultraviolet-visible (UV–vis) spectroscopy, revealing a large association constant of $1.4 \times 10^{11} \sim 1.1 \times 10^{12}$ M^{-1}. The

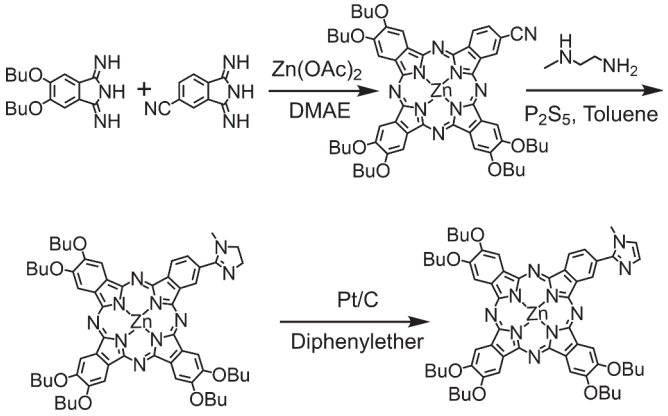

Figure 1.10 Synthesis procedures of hexa-*n*-butoxyimidazolynylphthalocyaninato zinc and hexa-*n*-butoxyimidazolylphthalocyaninato zinc.

nuclear magnetic resonance spectroscopy (NMR) results disclose the formation of the J-type Pc dimers, exhibiting excellent fluorescence. In 2000, a Pc pentamer was prepared through a one-step reaction of oxo(phthalocyaninato)titanium(IV) with 2,3,9,10,16,17,23, 24-octahydroxyphthalocyanine. The obtained compound was characterized by mass, electronic absorption, and magnetic circular dichroism spectroscopy [113].

Metal–ligand supramolecular oligomers made up of Pcs and other photoactive species have been assembled through coordination bonds, forming various donor–acceptor (D-A) systems for exploring their basic chemistry and photophysics. Ru(II) compounds show remarkable stability in solutions due to the robust metal–pyridyl connection. Due to the absence/presence of terminal CO complexation, mononuclear Ru(II)Pc precursors are coordinated with either one or two sides in the axial position, leading to the photoactive dinuclear and trinuclear D-A species. For instance, pyridyl-containing perilendiimides (PDIs) and fullerene (C_{60}) have been used to coordinate with Ru(II) macrocycles, forming D-A dimeric and trimeric compounds [23, 114–116]. In 2006, a novel donor–acceptor–donor (D-A-D) trimer hybrid was constructed by the axial complexation of two metallic Pcs [Ru(CO)Pc] with a PDI linker containing two 4-pyridyl substituents. [Ru(CO)Pc] was prepared by through the metalation of the tetra-*tert*-butylphthalocyanine to react $Ru_3(CO)_{12}$ in refluxing phenol with a yield of 80%. In addition, a PDI linker bearing two 4-pyridyl groups located on the imido position was produced by the reaction of 1,7-bis(3′,5′-di-tert-butylphenoxy)perylene-3,4:9,10-tetracarboxydianhydride with 4-aminopyridine with the help of $Zn(OAc)_2$. Single carbonyl coordination [Ru(CO)Pc] ensures the complexation of one PDI linker at the opposite axial site of two Pc molecules with a yield of 68% in chloroform. These monomeric compounds and trimeric arrays have been characterized by various spectroscopic methods. The photophysical properties of this D-A compound were determined, revealing the photo-driven generation of the long-lived radical ion pair states [Ru(CO)$Pc^{\bullet+}$-BPyPDI$^{\bullet-}$-Ru(CO)Pc] with a lifetime of 115 ns.

In 2016, new cart-wheel-type D-A-D hybrids were constructed by modifying the metals and peripheral substituents of Pcs and PDI for optimizing their photophysical behaviors (Figure 1.11) [115]. In addition to zinc/ruthenium carbonyl tetra-*tert*-butylphthalocyanine regioisomers, Zn(II) and Ru(II) Pc derivatives containing four and eight ferrocenes attached on the peripheral positions of macrocycles were prepared for constructing D-A-D hybrids. Suzuki cross-coupling reaction between 4-iodophthalonitrile and ferroceneboronic acid generated 4-ferrocenylphthalonitrile with a yield of 45%. The subsequent template cyclotetramerization of this precursor led to the formation of four ferrocene-substituted zinc/metal-free Pcs. Another analog ruthenium carbonyl Pc was prepared through the metalation of metal-free Pc and ruthenium dodecacarbonyl with a yield of 24%. For easy characterization and comparative study, symmetric octa-substituted metallic Pcs were also prepared. Therefore, 4,5-bisferrocenylphthalonitrile was afforded using Suzuki cross-coupling between 4,5-diiodophthalonitrile and ferroceneboronic acid. However, the electron-donating effect of ferrocene units prevents the successful template cyclotetramerization based on the above-described cyclotetramerization conditions. Instead, cyclotetramerization of the corresponding diiminoisoindolines was achieved with the help of hexamethyl disilazane, and the necessary metalation was employed to provide ruthenium carbonyl octa-substituted Pc. *N*,*N*′-Di(4-pyridyl)-1,6,7,12-tetrakis(4′-tert-butylphenoxy)perylene-3,4:9,10-tetracarboxylic acid bisimide [BPyPDI] was reacted with an excess of ruthenium carbonyl complexes in chloroform at room temperature to obtain the D-A-D trimers with a yield of 58–78%. The complexation of zinc Pc and BPyPDI in chloroform was carefully explored using the NMR technique. In particular, electronic communications between ferrocene units through Pc macrocycle (long distance across 11 bonds) were observed, and tiny electronic communications were also indicated between the Pc and PDI chromophores. Furthermore, the introduction of ferrocenes facilitates the fast energy transfer from the excited-state PDI to Pcs. In addition, these ferrocene substituents slightly accelerate the charge separation of the RuPc–PDI arrays upon photoexcitation of the PDI chromophore but significantly speed up charge recombination. Similar assembly and photophysical studies have been performed upon Pc-C_{60} supramolecular arrays made up of linear fullerene mono- and bispyridyl ligands to zinc/ruthenium Pcs [114, 116]. In addition to the coordination-driven oligomers, there are also supramolecular arrays constructed from Pc and functional chromophores through other weak interactions, such as hydrogen bonds and crown ether–alkyl ammonium cation interactions [117–120]. In this chapter, those supramolecular nanostructures including nanowires and nanoparticles, which are obtained from the self-assembly process and seem to have no well-defined structures, are not discussed due to lack of well-defined structures.

1.3.4 Phthalocyanine-Based Covalent-Bonded Oligomers

1.3.4.1 Phthalocyanine-Based Fused Oligomers

These Pc-based conjugates have attracted intense research interests due to a wide range of solar spectra and the efficient intramolecular energy transfer between

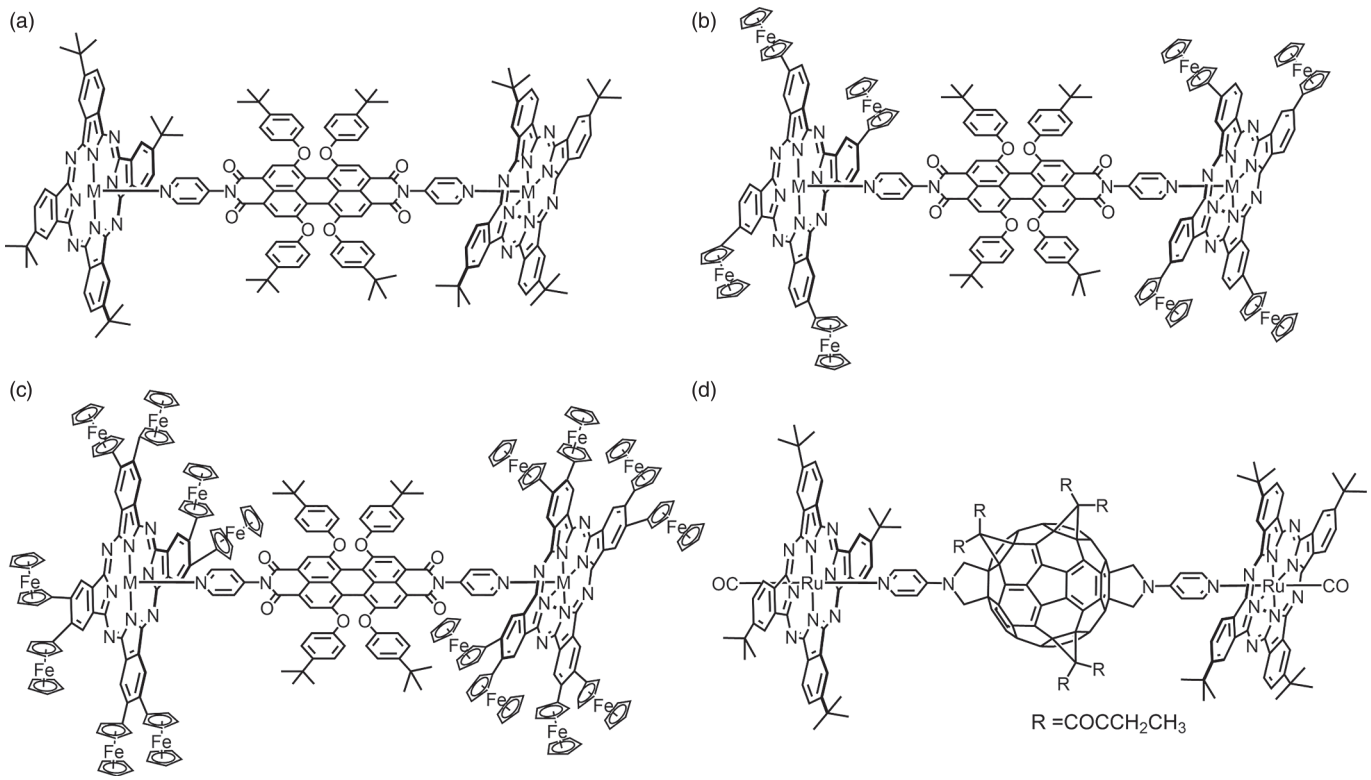

Figure 1.11 (a) Molecular structures of supramolecular triads MPc_2–perilendiimides (a–c) and $Ru(II)Pc_2$–C_{60} (d).

chromophores. Several groups are interested in the synthesis and spectroscopic and electrochemical characterization of fused oligomeric Pc-based systems. Binuclear Pcs with two macrocycle units bridged by a benzene ring are the famous representatives of planar covalent-linked Pc oligomers, possessing the extension of the conjugated π-system. Binuclear homoleptic Pcs bearing only one common benzene ring were reported in 1987 [121]. Thus far, binuclear zinc and magnesium Pcs have been prepared from the direct condensation of diiminoisoindoline/phthalonitrile and 1,3,5,7-tetraiminopyrrole[3,4-f]isoindoline in the presence of metal salts in high boiling point solvents. A 10-fold excess of phthalonitriles relative to 1,3,5,7-tetraiminopyrrole[3,4-f]isoindoline improves the higher yields of target binuclear compounds. During the reaction, the by-products include monomer Pc and different oligomers such as trinuclear linear and angular isomers in a trace amount. The treatment of binuclear magnesium Pcs with concentrated H_2SO_4 results in metal-free binuclear compounds. The solid-phase synthesis has been employed for the preparation of binuclear nickel complexes derived from phthalonitrile compounds and metal salt. Microwave radiation (MW) has been introduced in the solid-phase synthesis to enhance the yield of binuclear products in a short time of 5 minutes. For further extending the conjugation π-system, a binuclear Pc sharing a naphthalene ring, rather than a benzene ring, was reported in 1993 by using one-pot condensation of bis(diiminoisoindoline) and diiminoisoindoline [122]. In contrast, the absence of the template ion gives a low yield of metal-free species. The extension of the peripheral π-system has been established by constructing binuclear naphthalocyanines [123, 124]. These binuclear macrocycles have been used to prepare sandwich-type compounds, and the π-bridged delocalized biradical antiferromagnetic interaction plays an important role in the magnetic hysteresis for this compound [125].

Trinuclear and tetranuclear Pcs with much bigger conjugation system have been isolated as by-products of binuclear Pcs. The first trinuclear benzo-bridged π-electron-conjugated Pc was reported in 2007 [126]. It is worth noting that a novel Pc pentad has been designed and prepared by a stepwise method via asymmetric diiodide-substituted phthalocyaniato zinc compound, dicyano-substituted species, and then cyclotetramerization in boiling anhydrous *n*-pentanol with the help of a magnesium template. After the acidification treatment, a de-magnesium molecule has further been made as a water-soluble nanoparticle (Zn_4-H_2Pc/DP) with the surface modification of 1,2-distearoyl-sn-glycero-3-phosphoethanolamine–*N*-[methoxy(polyethylene glycol)-2000] (DSPE–PEG_{2000}–OCH_3) [127]. The obtained Pc nanoparticles exhibit an interesting absorption pattern in the near infrared (NIR)-II region with a large extinction coefficient at 1064 nm. Under the irradiation of 1064 nm laser, the high photothermal conversion efficiency and intense photoacoustic signal ensure the good biocompatibility and notable tumor ablation ability of nanoparticles. Similar to the above stepwise method, the bi-, tri-, and penta-nuclear-fused heteroleptic Pc–Por are derived from mononuclear A_3B-type dicyano-substituted Por monomers followed by cyclotetramerization with functional phthalonitriles [128–131] (Figure 1.12).

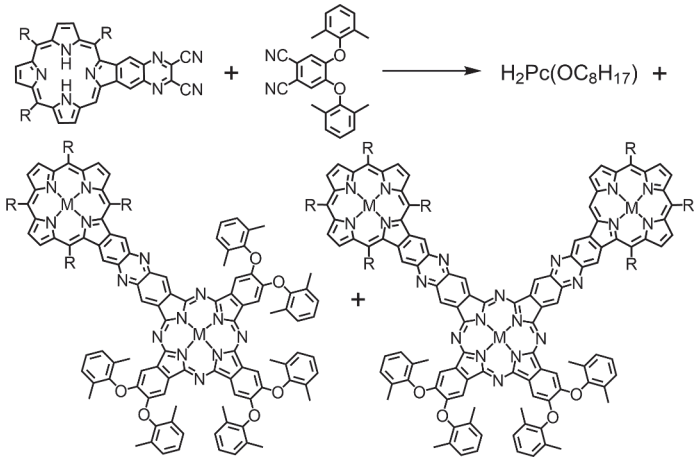

Figure 1.12 Synthesis of Pc–porphyrin-fused dimers and trimers (M = 2H and Zn).

In addition to conventional cyclotetramerization, a dinuclear pyrazine-bridged Pc has been created by the condensation reaction of unsymmetrical ABBB-type diamino-substituted Pc with a very high yield of 72%. This opens a new gate to design and prepare conjugated oligomeric Pc derivatives [132]. In 2017, a new approach by 2,3,9,10,16,17-hexakis(2,6-dimethylphenoxy)-23,24-diaminophthalocyaninato zinc(II) reacting with 2,7-di-tert-butylpyrene-4,5,9,10-tetraone and hexaketocyclohexane enabled the generation of the binuclear and trinuclear Pc-fused zinc complexes with a moderate yield of 13% and 25%, respectively [133]. Such strategy has been used to prepare fused Pc and Por dyad through the condensation reaction of 1,2-diamino-substituted zinc Pc and zinc 2,3-dioxoporphyrin in a mixture of $CHCl_3$/AcOH [134].

1.3.4.2 Phthalocyanine-Based Covalent-Linked Oligomers

Apart from the pursuit of the above fused multinuclear Pc-based systems with a large π-electron delocalized structure, the preparation of Pc to Pc through suitable linkages for operating the electronic interactions between chromophores was initiated as early as 1991. The first synthetic approach to prepare conjugated, binuclear Pcs with covalently linked alkyne and alkene groups was proposed by Leznoff et al [135]. By using this approach with the help of palladium-catalyzed reactions, many alkynyl- and alkenyl-bridged binuclear Pcs compounds have been created. For example, the Sonogashira cross-coupling reaction between a terminal alkyne-substituted Pc and a monoiodo-substituted Pc has afforded various binuclear species. In 2004, a zinc Pc dimer was prepared through the Sonogashira coupling reaction between unsymmetrical tri-*tert*-butyliodophthalocyaninato zinc(II) and tri-*tert*-butylethynylphthalocyaninato zinc(II) with a high yield of 70% (Figure 1.13) [136]. Interestingly, the cyclotrimerization of this dimer has been converted into a hexamer with six zinc Pcs decorated on a benzene ring in dry dioxane with the assistance of $Co_2(CO)_8$ catalyst. The cross-coupling methodology has been further developed to fabricate butadiynyl- and other conjugated group-linked

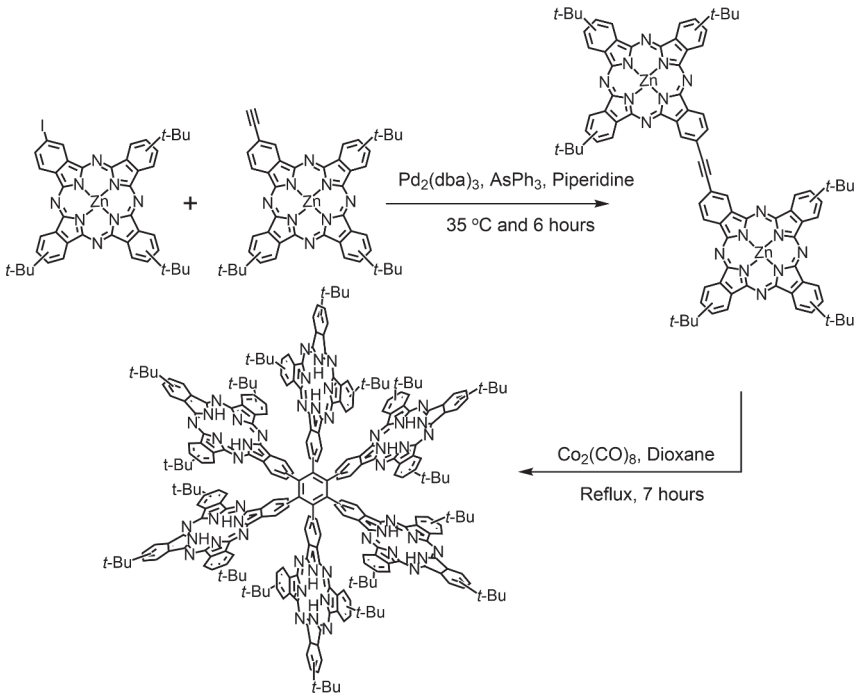

Figure 1.13 Synthesis of tri-*tert*-butyliodophthalocyaninato zinc(II) and tri-*tert*-butylethynylphthalocyaninato zinc(II).

compounds. Various Por–Pc oligomers and some D-A-type species such as Pc-C_{60} and Pc-perilendiimides (PDIs) and Pc-anthraquinone have been demonstrated to possess efficient intramolecular charge-separated states under excitation [137–143].

1.3.5 Cofacial and Cage-Like Phthalocyanine-Based Compounds

Different from the conventional planar Pc monomers and oligomers, those cofacial and cage-like species have unique void space and electronic coupling, leading to interesting spectroscopic and electrochemical properties beyond the monomeric compounds. Since the late 1980s, binuclear Pcs covalently linked through their benzo rings with different flexible bridges have been prepared and investigated [144]. The so-called cofacial (also called clamshell) systems are those species with two Pcs located on a scaffold in a face-to-face mode, which is different from those oxygen/nitrogen-bridged Pcs and supramolecular K^+/Ca^{2+}-bridged crown-substituted Pc aggregates. The first cofacial Pc dimer was produced in 1987, generating the binuclear Pcs linked on 1,8-naphthalene unit (Figure 1.14) [145]. For details, heterocoupling reaction of 4-iodophthalonitrile with 1,8-diiodonaphthalene with the help of nickel powder to afford 1,8-bis(3,4-dicyanophenyl)naphthalene. The subsequent transformation into the corresponding dihydroisoindole has been performed for the tetracyclization with dihydroisoindole derived from 4-neopentyloxyphthalonitrile, leading to the

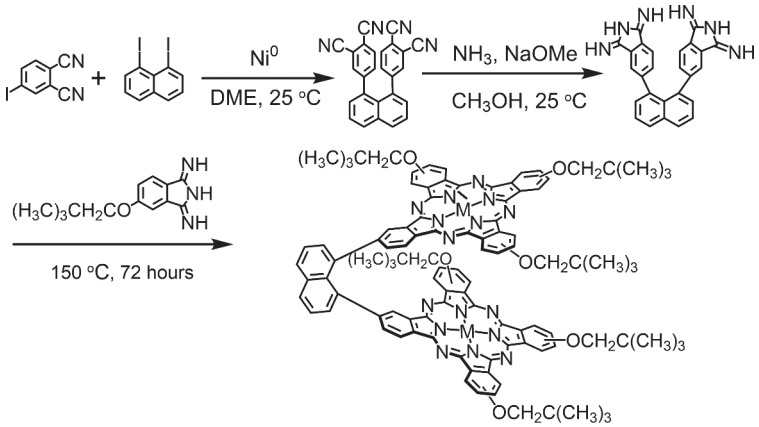

Figure 1.14 Synthesis of 1,8-bis-2′-(9′,16′,23′-trineopentyloxyphthalocyaninyl)-naphthalene.

metal-free 1,8-bis-2′-(9′,16′,23′-trineopentyloxyphthalocyaninyl)naphthalene in a moderate yield. The dinuclear cobalt, copper, and zinc derivatives were also prepared by the metalation of the above metal-free compound. These cofacial Pcs exhibit interesting sensing properties. For example, binuclear Pcs are anchored on a calixarene scaffold, forming a Pacman-type compound with potential chemoreceptor applications [146]. This compound was obtained from the Li-template reaction of the bis(phthalonitrile)-substituted calixarene with an excess of phthalonitrile in penthanol at 110 °C. The unique recognition of heavy metal ions such as Ag^+ and Hg^+ through UV–vis spectrum is due to the binding between Pc rings and metal ions.

Ball-type Pcs are a new class of complexes with cage-like molecular structures, which were first introduced by Tomilova in 2002 [147] and well developed by Bekaroğlu [148]. These compounds have common characteristics, possessing four linkers to bridge the peripheral positions of different isoindole units from two face-to-face Pcs. In these molecules, the synthesis and properties of ball-type Pcs have been developed by changing either metal centers or cross-linkers. The employment of diverse linkers, including calix[4]arene, 4,4′-isopropylidendioxydiphenyl ligands, pentaerythritol bridges, and so on, is capable of adjusting the distance between the cofacial Pc rings and integrating various functions beyond Pc monomers. The presence of distance-dependent interaction between the two cofacial Pcs or neighbor metal centers in this type of compound has been determined using spectroscopic and electrochemical techniques. Typically, these ball-type molecules are stepwise assembled from the substitution of 4-nitrophthalonitrile on a functional scaffold and followed by the cyclotetramerization reaction [149]. The used precursors enumerate 1,2-bis(3,4-dicyanophenoxymethyl)-benzene [150], calix[4]arene [151], squaric acid [152], 4,4′-(hexafluoroisopropylidene) diphenol [153], and silsesquioxanes [154]. Ball-type molecules are prepared like those monomeric under solution, in solid phase and under microwave irradiation conditions, having moderately low yields. These functional molecules have many

potential applications, including gas sensors [155], third-order nonlinear optical devices [156], photodynamic therapy [157], and electrocatalysis [153].

Due to the synthetic difficulty and planar molecular structure of Pcs, it is difficult to prepare molecular building blocks for the cage-like molecules in addition to the cofacial structure. In 2018, an M_2L_3 metallo-Pc cage was reported, serving as a new host for electroactive molecules. For details, a bidentate C_{2v} Pc ligand (*syn*) was prepared and purified from the mixtures, and it (3 equiv.) was reacted with 2-formylpyridine (6 equiv.) and iron(II) trifluoromethanesulfonate $Fe(OTf)_2$ in CD_3CN for 24hours at room temperature under a nitrogen atmosphere, leading to the formation of metallo-Pc cage $Fe^{II}{}_2Pc_3(OTf)_4$.

The self-assembled structure was determined by various spectroscopies. In particular, this helicate-like cage as a host has been used for the complexation of fullerenes species and naphthalenediimide derivatives, displaying the photoactivated electronic interactions between host–guest components [158]. In contrast to Pc-based cages, several subphthalocyanine-based metallosupramolecular capsules have been self-assembled through a metal–py coordination moiety possibly due to the easier production of corresponding ligands (Figure 1.15). [159] Only [4 + 2] Pc-based POCs have been reported in 2023, and they were obtained from the self-assembly of a 2,3,9,10,16,17,23,24-octahydroxyphthalocyaninato zinc(II)/Ni(II) (MPc-$(OH)_8$, a rod-like 1,1′ : 4′,1′′-terphenyl]-2,2′′,3,3′′-tetrol (Tp-4OH), and boric

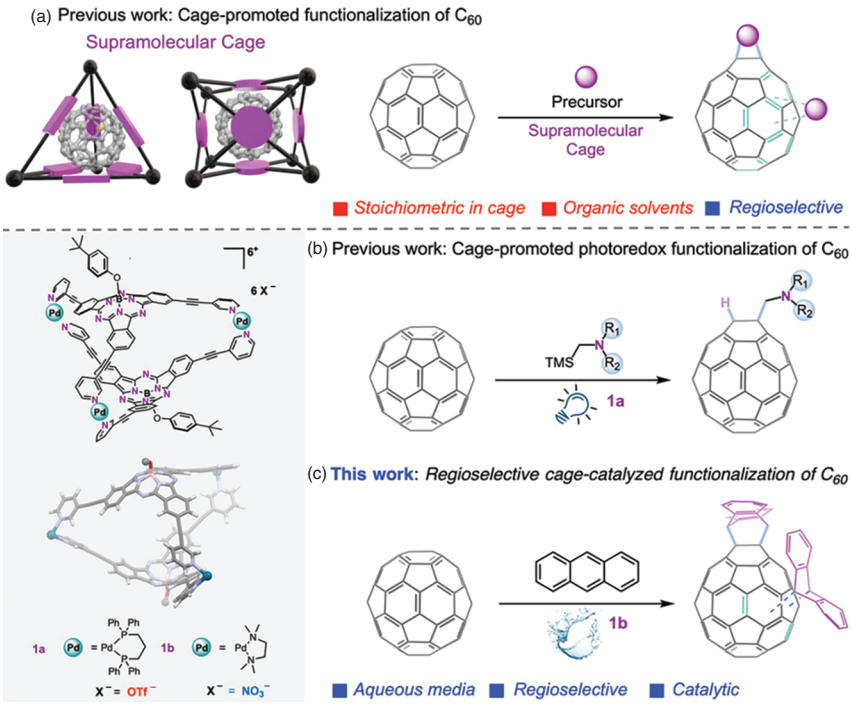

Figure 1.15 Cage-promoted transformations of fullerenes. Source: Reproduced from Ref. [159] / with permission of John Wiley & Sons.

acid in polar solvents. The increase of reaction temperature to 150 °C promotes the production of cage at a yield of 70% [160].

1.4 Phthalocyanine-Based Polymeric Materials

For primarily studying the interesting chemical and physical behaviors as well as the potential applications, some Pc-based oligomers have also been established by the covalent and non-covalent interactions, such as coordination and hydrogen bonds. These systems are regarded as the intermediate to bridge the monomer molecules and the polymeric materials. In the following section, those crystalline materials including functional molecular crystals, coordination polymers, and COFs have been primarily present, and the amorphous porous organic macromolecules and polymers also have been summarized briefly.

1.4.1 Phthalocyanine-Based Porous Molecular Crystals

In the context of porous molecular crystals, the well-defined supramolecular polymeric structures have been engineered and accessed by the recrystallization of discrete organic building blocks. In parallel to exploring the practical advantages of zeolites and activated carbons with porous structures, the investigation that offers new porous organic-based microporous counterparts with in-built functionalities toward heterogeneous catalysis, adsorption, and separations is of significant interest. Although the highly functional Pcs resemble Por macrocycles from the level of the rigid planar structures, they have been rarely used to build diverse crystalline nanoporous materials due to the synthesis challenge. Actually, these Pc macrocycles possess a strong tendency to generate dense self-association aggregates due to the extended planarity, preventing engineering nanoporous materials. As a result, the substituents and accessible coordination metal ions have been introduced to either create severe steric effects at the peripheral location of the Pc core or deviate from the planar macrocycles. Pcs and octaazaphthalocyanine derivatives (azaPcs) have been used as building blocks for the assembly of nanoporous molecular crystals since 2005 [161, 162]. McKeown et al. reported a 2,3,9,10,16,17,23,24-octa(2′,6′-diisopropylphenoxy)phthalocyaninate zinc complex (ZnPc′), where the recrystallization of this compound in $CHCl_3$ via the acetone diffusion method provides structurally porous molecular crystals disclosed by SCXRD study (Figure 1.16). The central Zn^{2+} ion is coordinated with four nitrogen atoms from the Pc core and a water oxygen atom, forming a pyramid coordination geometry. The eight peripheral 2,6-diisopropylphenoxy substituents exert an important role in changing the conventional cofacial arrangement of the Pc, leading to a porous cube with a minimum open diameter of 2.33 nm and a pore volume of more than $8nm^3$. These porous cubes are interconnected via narrow cylindrical channels with a pore size of 0.4nm at each corner. The calculations with the PLATON program suggest that the solvent-accessible void volume is 38.2% of the total volume, which consists of disorder acetone and water molecules filled in the pores.

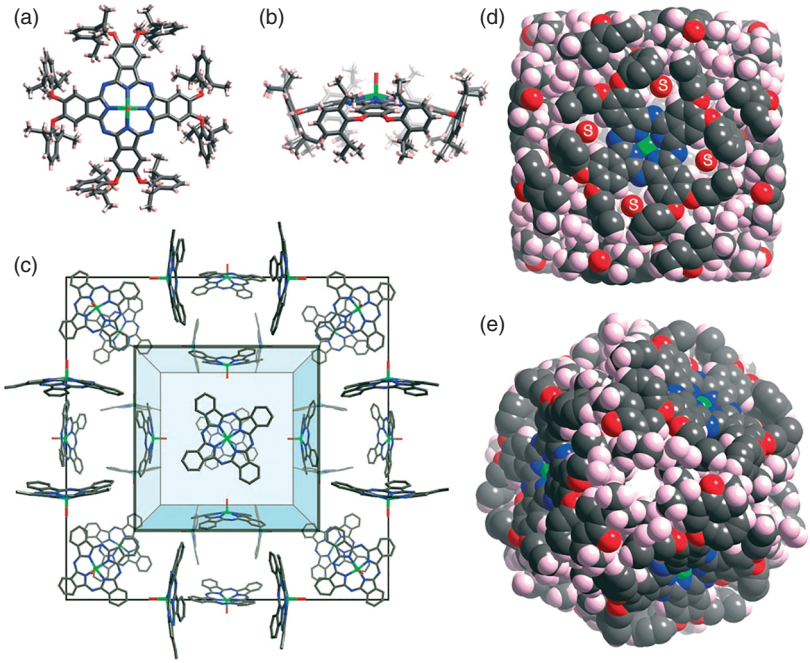

Figure 1.16 The molecular and crystal structure of ZnPc′. Source: Reproduced from Ref. [161] / with permission of John Wiley & Sons.

SCXRD and NMR spectroscopic results disclose that the crystal structure of porous crystals with big void is very stable during the solvent exchange of $[D_6]$acetone, methanol, and water. After removal from the crystallization solution, the porous crystal is collapsed by the solvent escape due to the disappearance of powder X-ray diffraction (PXRD) signals. In the long term, it is difficult to get highly nanoporous molecular crystals with permanent porosity indicated by solvent and vapor sorption measurement due to the fragile connection. Sophisticated crystal engineering provides a good opportunity in this context.

Until 2010, McKeown et al. reported a derivative of iron Pc, 2,3,9,10,16,17,23, 24-octa(2′,6′-diisopropylphenoxy)phthalocyaninate iron(II) compound [$(dipPhO)_8$ PcFe] [163]. The simple crystallization of this compound gave an isostructural crystal of the zinc species, denoted as PNC[*c*BuNC-Fe-*v*BuNC]. This is also true for other metal Pc derivatives [$(dipPhO)_8$PcM] (M = Mg^{2+}, Al^{3+}, Ti^{4+}, Mn^{2+}, Co^{2+}, Ru^{2+}, and In^{3+}). Rapid exchange of the axial ligands such as *t*-butyl isocyanide (BuNC) upon this series of nanoporous molecular crystals was demonstrated by a single-crystal to single-crystal (SCSC) transformation by adding a solution of py, *N*-methylimidazole, imidazole (im), 4,4′-bipyridyl (bipy), or 1,4-phenylenediisocyanide (pdic). The longer ligands (bipy and pdic) are able to bind two adjacent metal ions across the cavity. Interestingly, exposure of PNC[*v*BuNCFe-*c*bipy-Fe-*v*BuNC] and PNC[*v*BuNC Fe-*c*pdic-Fe-*v*BuNC] induces the replacement of BuNC with N_2. In contrast, the py ligand of PNC[*v*py-Co-*c*bipy-Co-*v*py] was removed to form [Co-*c*bipy-Co].

These three phases retain their crystal structures according to PXRD analysis, ensuring the significant nitrogen adsorption at $P/P^0 < 0.2$ and the high surface area in the range of 850–1000 m^2 g^{-1} deduced from these isotherms. In 2019, it was found that a simple co-crystallization of a fullerene (C_{60} or C_{70}) and a [$(dipPhO)_8PcCo$] forms porous molecular crystals of PNC[$c C_{60}$/Co–$v H_2O$] and PNC[$c C_{70}$/Co–$v H_2O$] [164]. Fullerenes are filled cavities formed by the concave Pc surfaces, and water molecules occupy the axial position of metallophthalocyanines (MPcs). The isostructural co-crystals of PNC[$c C_{60}$/Cu–$v H_2O$], PNC[$c C_{60}$/Ag–$v H_2O$], and PNC[$c C_{60}$/H_2–$v H_2O$] consist of $(dipPhO)_8PcM$ (M = Cu, Ag, and H_2). Furthermore, the presence of open channels for small molecules to bind with metal centers has been verified by SCSC transformation of water with py. The pressure-induced change in crystal structure was investigated using synchrotron SCXRD. In addition, the inclusion of fullerenes stabilizes the porous structure after solvent removal, exhibiting the permanent porosities for PUNC[$c C_{60}$/Co] as confirmed by in situ SCXRD and gas sorption. At the end of this paragraph, in addition to those co-crystals made up of monomeric Pc and C_{60}, the sandwich-type compounds have been used to co-crystallize with fullerene to adjust the single-molecule magnetic properties, photo-driven charge transfer properties, and organic field-effect transistor behaviors [165–168]. There are also interesting porous molecular crystals made up of biprotonated dodecaphenylporphyrin (H_4DPP^{2+}), 1,4,8,11,15,18,22,25-octaphenylphthalocyaninato zinc [Zn(OPPc)], and 4-pyridinecarboxylate anion. The nitrogen atom of 4-pyridinecarboxylate anion binds with the Zn ion of [Zn(OPPc)], and its carboxylate group interacts with H_4DPP^{2+} through intermolecular hydrogen bonding interactions. The molecular volume was calculated as 5096 $Å^3$ on the basis of its crystal structure. Photoexcitation of the supramolecular assembly in solution induces intra-supramolecular electron transfer state, accompanied with the generation of one electron-reduced diprotonated Por and one-electron-oxidized ZnPc radicals [169].

1.4.2 Phthalocyanine-Based Coordination Polymers

Among various supramolecular polymeric compounds, coordination polymers are well known as a kind of important crystalline functional materials. They are constructed by the coordinate interactions, directing the high-order organization of discrete metal ions/clusters and organic linkers. Such inorganic and organic multicomponent systems have attracted intense research interests due to the multifunctional integration in a matter based on fundamental magnetic, photonic, and electronic modules as well as their heterogeneity advantage in the application in the field of catalysis (Figure 1.17) [170, 171]. The first Pc-based coordination polymer with a crystal structure was reported in 1994. The reaction between tetracyanoethylene (TCNE) and manganese phthalocyanine (MnPc) led to the formation of two coordination polymers α-[MnPc][$TCNE]_{0.5}$ and β-[MnPc][$TCNE]_{0.5}$ under grinding followed by dissolution in MeCN and reflux in MeCN, respectively. SCXRD investigation discloses the one-dimensional (1D) chain for β-[MnPc][$TCNE]_{0.5}$. The magnetic properties of these two phases have been investigated. With

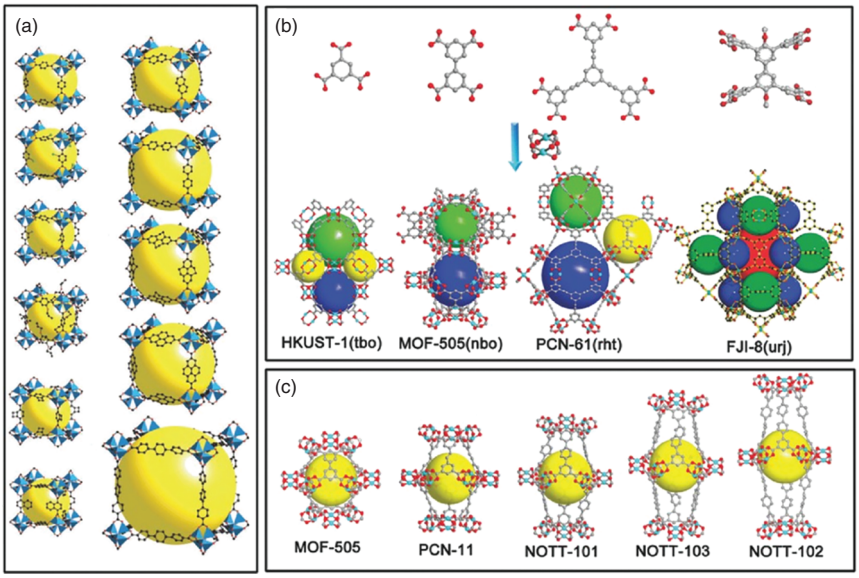

Figure 1.17 (a) Crystal structures of IRMOF-n with general formula $Zn_4O[R(COO)_2]_3$. (b) Various organic ligands with $Cu_2(COO)_4$ secondary building unit to construct copper(II) MOFs and (c) tunable pore structures of **nbo**-type MOFs. Source: Reproduced from Ref. [171] / with permission of John Wiley & Sons.

the axis coordination, there are another two 1D coordination polymer single crystals. [172, 173] In the 1990s, MOFs were established by connecting inorganic metal/cluster and organic linkers through coordination interactions, which are also called porous coordination polymers [174]. MOFs possess highly porous structures, synthetic advantages, organic–inorganic hybrid nature, and diverse applications and have more variety and multiplicity in synthesis, structures, and functions than other crystalline porous materials. These coordination polymeric materials have also ensured the occurrence of post-synthetic organic and inorganic reactions on their frameworks while maintaining porosity or crystallinity. To date, the principles of molecular pre-design and post-synthetic modification have been synergistically employed to engineer these framework materials for attaining useful and multi-faceted properties and functions, and the current research focuses on exploring the relationship between structures and physical properties, chemical reactivity, and a variety of applications, which is an important set for practical materials.

Given the fact that Pors play an important role in essential natural processes including light harvesting, catalysis, and electron and oxygen transfer, carboxyl- and py-containing Pors have been assembled as early as the 1990s [170, 175]. However, the first Por-based MOF with permanent porosity was established in 1999 [176]. In contrast to the well-developed Por-based MOFs with a plethora of 1D, two-dimensional (2D), and three-dimensional (3D) examples [177], only a few Pc-based MOFs have been present since 2018 due to the difficulty in the synthesis of eight-connecting symmetric macrocycles and matching with suitable metal secondary

building units. In 2018, the first report of a Pc-based MOF [Cu_2(PcCu-O_8)] was fabricated from the reaction of 2,3,9,10,16,17,23,24-octahydroxy-phthalocyaninato copper(II) [CuPc$(OH)_8$] with copper(II) trifluoroacetylacetonate [$Cu(CF_3acac)_2$] in the presence of ammonia and DMF at 120 °C for 36 hours. The crystalline and porous structure of [Cu_2(PcCu-O_8)] was determined by PXRD and gas sorption measurements. The **sql** topological AA-packing 2D MOF in the black powder state was obtained, displaying an electrical conductivity of 1.6×10^{-6} S cm^{-1} at 80 °C. Employment of this Pc MOF as a cathode of lithium-ion battery (LIB) delivers large charge/discharge capacities of 151/128 mA h g^{-1} and excellent stability after 200 working cycles. Such outstanding LIB performance is associated with the electrically conductive and redox-active framework of porous 2D MOF. In the same year, Jia et al. produced the first Pc-based 2D MOF [Ni_2(NiPc$(NH)_8$)] based on the reaction of 2,3,9,10,16,17,23,24-octaamino-phthalocyaninato nickel(II) [NiPc$(NH_2)_8$] with $NiCl_2 \cdot 6H_2O$ in DMSO with the help of ammonia at 60 °C for 12 hours [178]. This blue-black [Ni_2(NiPc$(NH)_8$)] films with a thickness of 100 ~ 200 nm were grown on various substrates, including fluorine-doped tin oxide (FTO), indium tin oxide, quartz glass, and silicon wafer. The electrical conductivities of the films on quartz were up to 0.2 S cm^{-1} at room temperature. In addition, [Ni_2(NiPc$(NH)_8$)] films deposited on FTO were applied as electrocatalysts for water oxidation catalysis, exhibiting outstanding oxygen evolution reaction (OER) activity under alkaline conditions. Herein, it is worth noting that *ortho*-phenylenediamine and catechol derivatives have the same capability in forming square-planar complexes through the complexation with metal ions, leading to the square-planar node. This, in combination with the correspondingly rich and reversible redox forms, injects the new momentum for functional Pc MOFs with excellent charge transfer, catalytic, and sensing properties. In 2023, the assembly of 2,3,9,10,16,17,23,24-octathiolphthalocyaninato copper(II) [CuPc$(SH)_8$] with Ni^{2+} afforded a highly crystalline Pc-based MOF [Ni_2(PcCu-S_8)] containing nickel-bis(dithiolene) (NiS_4) coordination linkages. This MOF was applied in the supercapacitors in 1 M $TEABF_4$/acetonitrile. Its good pseudocapacitive properties are associated with the reversible accommodation of two electrons upon each functional NiS_4 unit, showing a high specific capacitance of 312 F g^{-1} as well as outstanding cycling stability after 10 000 runs.

The eight-connected fourfold symmetry of the above three Pc derivatives was induced by the bis(dioxolene), bis(*o*-diiminobenzosemiquinonate), bis(dithiolene) complex linkages to form 2D homo/heterometallic MOFs with **sql** topology. Only one single crystal Pc, [MOF-1992·$(Fe)_3$], was constructed from the solvothermal reaction of $FeCl_2$ and 2,3,9,10,16,17,23,24-octahydroxy-phthalocyaninato cobalt(II) [CoPc$(OH)_8$] in N,N-dimethylformamide/water/methanol (100/0.5/0.5, v/v) at 150 °C for 16 hours [179]. Catechol-bridged Fe trimers as nodes assemble [CoPc$(OH)_8$] to afford [MOF-1992·$(Fe)_3$] with a 3D porous **roc** topological architecture. Three Fe^{3+} play the role of balance ion filled in the pores of the $[Fe_6(OH_2)_4(CoPc\text{-}O_8)_3]^{6-}$ framework. The cathodes made up of MOF-1992 and carbon black exhibit a current density of −16.5 mA cm^{-2} and an overpotential of −0.52 V for the CO_2 reduction reaction in water, leading to CO Faradaic efficiency (FE_{CO}) of 80%. Among 6 hour

lasting measurements, this MOF cathode achieves a turnover number of 5 800 with a turnover frequency of 0.20 s^{-1}.

The nanoscale MOFs are a good platform to support various functional molecules using pores and accessible anchors [180, 181]. Their excellent structural tunability, crystallinity, framework rigidity, high porosity, and biodegradability arouse wide research interests (Figure 1.18). Herein, two examples presented by Lin are introduced [182, 183]. Zinc(II) 2,3,9,10,16,17,23,24-octa(4-carboxyphenyl)Pc [$ZnPc(COOH)_8$] photosensitizer was spatially confined in the channels of a nanoscale MOF Hf_{12}-QC (QC = 2″,3′-dinitro-[1,1′,4′,1″,4″,1‴-quaterphenyl]-4,4‴-dicarboxylic acid). The generated [ZnPc-$(COOH)_8$@Hf-QC] effectively improved the reactive oxygen species (ROS) generation under light irradiation due to the decreased molecular aggregation. With higher cellular uptake, enhanced ROS generation, and better biocompatibility, ZnP@Hf-QC was applied photodynamic therapy, showing a half-maximal inhibitory concentration (IC_{50}) of 0.14 μM. In particular, this nanoscale Pc-doping MOF shows a prominent antitumor efficiency of >99% tumor growth inhibition and good cure rates of 80% toward two murine colon cancer models. Post-synthetic modification ensures that [$ZnPc(COOH)_8$] photosensitizers were coordination-anchored on Hf_{12} cluster nodes a nanoscale metal-organic layer based on $Ir(DBB)[dF(CF_3)ppy]^{2+}$ ligands [DBB = 4,4′-di(4-benzoato)-2,2′-bipyridine; $dF(CF_3)ppy$ = 2-(2,4-difluorophenyl)-5-(trifluoromethyl)pyridine]. The ultrathin positively charged nanoscale MOFs together with the generation of ROS upon the irradiation of dispersed [ZnPc $(COOH)_8$] photosensitizer allow the efficient mitochondria-targeted PDT. There are some amorphous Pc coordination polymers for catalysis and biomedicines. A representative example composed of MPc coordination layer/polyoxometalate (POM) was present in this section [184]. Cobalt tetraaminophthalocyanine (CoTAPc) was assembled with zinc ion and $H_3PMo_{12}O_{40}{\cdot}xH_2O$ (PMo_{12}) in the presence of polyvinylpyrrolidone under solvothermal conditions. The POM was introduced between Pc coordination layers to form Zn-CoTAPc/PMo_{12} composite nanosheet

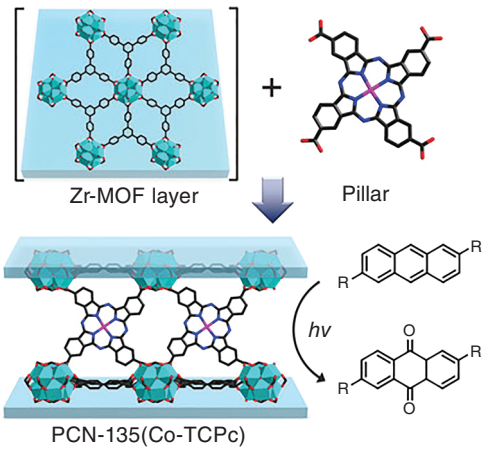

Figure 1.18 The synthesis procedure of the PCN-135 with Zr_6-BTB layer and Pc as the secondary building blocks. Source: Reproduced from Ref. [180] / with permission of John Wiley & Sons.

(NS) with a thickness of around 1.2 nm, exposing more active sites for CO_2 reduction photoelectrochemical catalysis. In the dark, this composite electrode shows a FE_{CO} of 96.1% at −0.7 V vs. RHE, with a corresponding turnover frequency (TOF) of 987 h^{-1}. Such CO_2 reduction activity was further enhanced under external light irradiation.

1.4.3 Phthalocyanine-Based Organic Polymers

In addition to coordination polymers, it is noteworthy that covalent organic polymers represent another class of important polymeric materials with robust architectures together with thermal and chemical stability [185, 186]. In this direction, COFs have been established since 2005 to extend discrete molecular modules composed of light elements into covalently connected structures through organic reactions [187, 188]. The chemistry of frameworks, with MOFs and COFs as important constituent components, was further advanced in comparison with Lewis' concept from the atom to the molecule [189, 190], by precisely controlling and manipulating the alignment and distribution of the molecular matters through metal complexation and covalent organic reactions, respectively. In this section, the selected paradigms of covalent organic polymers, dendrimers, and COFs are also the subject due to their potential applications.

1.4.3.1 Amorphous Phthalocyanine-Based Organic Polymers

The Pc macrocycles have been used as building blocks to design and prepare robust, processable covalent-linked organic polymeric materials. As mentioned in Section 1.2, the monomeric Pc macrocycle possesses up to 16 active sites on the peripheral positions for covalent linkage with organic polymer and two potential axis sites for covalently bonding with the center atom. As a result, the molecular orientation of the Pc units is fixed through strong covalent bonds [191]. According to the way in which the Pcs are covalently linked in the macromolecular polymers, these Pc organic polymers are classified as network, main chain, and side-chain species.

Preparation of polymeric Pcs offers the attractive prospect of dyes and pigment applications [192–194]. Network polymers were established by Marvel in the late 1950s [195, 196]. The cyclotetramerization of bis(phthalonitrile) or a bis(phthalic anhydride) bridged by a heteroatom (oxygen, sulfur, and selenium) as precursors under suitable conditions generates a dark-blue insoluble powder, which is difficult for characterization using solution methods [197]. It is worth noting that the abundant defects including triazine and isoindoline groups should be included in these polymers, although repeated washing and Soxhlet extraction with organic solvents are performed. Nitrophthalonitrile as a starting material prefers the nucleophilic aromatic substitution with the phenoxy groups of corresponding bisphenols to afford diverse precursors for polymeric Pc polymers established by Wöhrle. The employment of Cu or $CuCl_2$ seems to be helpful in the formation of uniform polymers containing a high metal content. However, heterogeneity of polymers is caused due to the generation of a Pc unit with different molecular symmetry. Following the increase of linker length between the Pcs, Pc-based polymers should

lead to open cavities and channels, and their optical and electronic properties have been studied due to the change of the relative orientation and distance of the adjacent Pc moieties. The cyclotetramerization reaction of a crown ether-linked bis(phthalonitrile) generates network polymers in the presence of various metal salts and quinoline at 200 °C, representing the first case consisting of uniform octa-substituted Pc units [198, 199]. The detailed development of Pc-containing polymers in the past 30 years before 2000 has been summarized [200]. Obviously, these Pc-containing polymers are constructed from the cyclotetramerization of bis(phthalonitrile) or a bis(phthalic anhydride), leading to networks with the surface area below $\sim 2\,m^2\,g^{-1}$ as determined by nitrogen adsorption [201]. This may be caused due to the serious completion of non-covalent self-aggregation of the Pc units to form nonporous dense structures. Until 2002, network polymers containing different metals with large surface areas of 450–950 $m^2\,g^{-1}$ were prepared from the spirocyclic-linked bis(phthalonitrile) monomer. The rigid spirocyclic linker makes adjacent Pc units into an orthogonal orientation, creating more porosities. This bis(phthalonitrile) with high yield was easily achieved through the aromatic nucleophilic substitution reaction of 4,5-dichlorophthalonitrile with 5,5′,6,6′-tetrahydroxy-3,3,3′,3′tetramethyl-1,1′-spirobisindane [202]. In 2011, a polymer of intrinsic microporosity based on a Pc component was created, showing a Brunauer–Emmett–Teller (BET) surface area of 806 $m^2\,g^{-1}$. The Diels–Alder reaction of 2,3,6,7-tetramethoxy-9,10-diethyl anthracene with 1,2,4,5-tetrabromobenzene in the presence of *n*-BuLi afforded dibromotriptycene derivative, which was further converted to dicyanotriptycene compound based on Rosenmund–von Braun reaction. Employment of this precursor formed the triptycene-substituted Pc. This demethylated Pc monomer reacted with 2,3,5,6-tetrafluoroterephthalonitrile to produce a green powder, which was characterized using the ^{13}C solid-state NMR spectrum and elemental analysis [203].

In 1960, the cyclotetramerization of 1,2,4,5-tetracyanobenzene in the presence of cuprous chloride afforded a 2D copper polyphthalocyanine. The adjacent 18-π electron aromatic systems are bridged through a benzene ring to form a conjugated network, obtaining high mobility ($1 \times 10^{-3}\ m^2\ V^{-1}\ s^{-1}$) and a narrow band gap of 0.26 eV [204]. Detailed investigations were carried out to optimize the reaction conditions, to make film, and to characterize the polyphthalocyanine by modern techniques before 2000. Because these rigid and planar 2D-conjugated polyphthalocyanines are insoluble, conventional solution polymerization and characterization techniques seem to be inappropriate. In 2011, the first well-ordered single sheet of polyphthalocyanine was reported using in situ characterization of scanning tunneling microscopy. Such polymeric arrays were grown onto Au(111) and Ag(111) as well as a thin insulating film of NaCl/Ag(100) surface by co-evaporation of Fe and 1,2,4,5-tetracyanobenzene in ultra-high-vacuum conditions at 360 K. This π-conjugated single sheet is also a 2D electron system with magnetic metals spread regularly in a planar lattice (Figure 1.19) [205, 206]. With the inspiration of the formation of polyphthalocyanine single NS, the first well-order polyphthalocyanine with PXRD analysis was reported in 2017. Copper octacyanophthalocyanine was prepared from the tetracyclization of 1,2,4,5-tetracyanobenzene in the presence

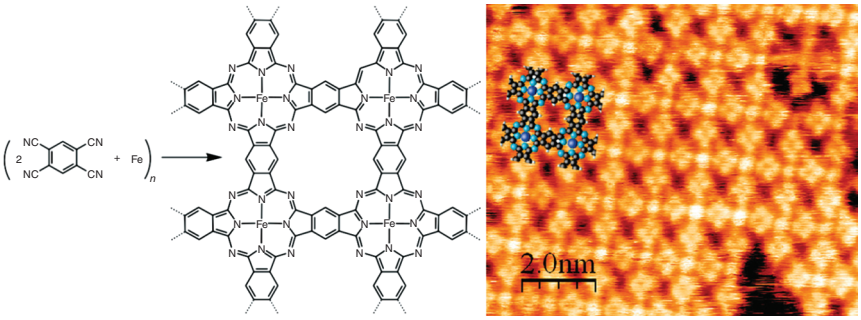

Figure 1.19 Synthesis and STM (scanning tunneling microscopy) image of the 2D iron polyphthalocyanine. Source: Reproduced with permission from Ref. [205] / American Chemical Society.

of $CuCl_2 \cdot 2H_2O$ at 240 °C for 4 hours with the help of sulfolane diazabicycloundecene, which was further applied to the solid-state transformation of copper octacyanophthalocyanine and $CuCl_2 \cdot 2H_2O$ in either the presence or absence of 1,2,4,5-tetracyanobenzene sealed in glass ampoules [207]. The crystal structures of the obtained materials were investigated using PXRD and transmission electron microscopy (TEM) methods, displaying the 2D square grid structures. Due to the excellent stability, physicochemical and catalytic properties, and easy production of these 2D-conjugated polyphthalocyanine, these materials with/without crystallinity have been widely investigated in the presence of electro- and photo-catalysis [208].

Main chain polymers are connected based on the Pc macrocycle monomers. However, the construction of these materials based on asymmetric Pc monomers is still challenging due to the complicated cyclotetramerization of mixed precursors. In 1994, the non-peripherally substituted AAAB-type Pc monomer was fabricated from the mixed phthalonitrile precursors, of which one bears two protected alcohol groups. This compound was used to react with oxalyl chloride, and further an equivalent monomer was added to form a polymer. Integration of the typical NMR signal indicates the formation of a simple linear main chain polymer with an average of ca. 10 Pc units [209]. In 2008, zinc tetra(2,4-dichloro-1,3,5-triazine)aminophthalocyanine (Zn-TDTAPc) was fabricated, which was implanted on poly(*N*-isopropylacrylamide) (PNIPAAm) through the covalent bonding, leading to a main chain polymer (Zn-TDTAPc-g-PNIPAAm). This polymer has good solubility, thermosensitive property, and high photoactivity in water and in most organic solvents [210]. The cofacially linked stacked polyphthalocyaninatometalloxanes $[PcMO]_n$, (M = Si, Ge, Sn), as a representative of main chain polymers has been investigated mainly due to their interesting electrical properties. These compounds were created in 1960 [211]. The $PcMC1_2$ compounds can be directly prepared from conventional methods, which hydrolyze $PcMCl_2$ to form $PcM(OH)_2$. The polycondensation of these compounds could be achieved in a vacuum at 325–440 °C or by heating it in refluxing 1-chloronaphthalene or quinoline [212]. These μ-oxo-linked central atoms in Pc units form 1D polymers with a small interplanar distance between the Pc units. Various characterization

exploration techniques including chemical, radiochemical, spectroscopic, diffractometric, and electron microscopic techniques reveal their highly regular, crystalline structures. For example, $[PcSiO]_n$ has excellent chemical stability due to the shielding effect of Pc macrocycles to prevent the approaching of reactants to the μ-oxo linkage. Amazingly, it has a self-dissociation in cold concentrated sulfuric acid without the detection of decomposition. To realize the high conductivity, either "heavy" oxidation (p-doping) or reduction (n-doping) should be performed to generate charge carriers [213, 214].

In contrast to main chain polymers, the side-chain polymers have the laterally attached Pc macrocycles, which are usually prepared through three methods, namely, (i) the direct grafting of a Pc onto a selected polymer. As early as in 1990, this approach was applied in the industrial coloration of cotton (cellulose) by grafting Pc dye with a reactive triazine unit, enabling the adsorption of polyaromatic hydrocarbons from polluted water [215]. In 2015, Pc-based side-chain copolymers were obtained through atom transfer radical polymerization (ATRP) and then modification by an azide–alkyne Huisgen cycloaddition, namely click reaction. The reaction of hydroxyl group-containing Pc with 6-chloro-1-hexyne formed alkyne-bearing Pc. In addition, the azide-terminated poly(methyl methacrylate) N_3-PMMA was prepared via ATRP using an azide-bearing ATRP initiator. The Pc-containing copolymers were constructed by the click reaction of the as-prepared polymers with an alkyne-bearing Pc compound [216]. (ii) The mixed cyclotetramerization of a polymer-bearing precursor. In 2015, a styrene monomer bearing a phthalonitrile group (VBOP) was constructed from a nucleophilic substitution reaction of 4-vinylbenzyl chloride with 4-hydroxyphthalonitrile. VBOP and styrene were polymerized into a copolymer based on a reversible addition–fragmentation chain transfer mechanism with the help of 2-cyano-2-propyl benzodithioate as a chain transfer agent and 2,2′-azobis(2-methylpropionitrile) as an initiator. The addition of CuCl and phthalonitrile in benzyl alcohol is beneficial for the formation of Pcs. However, the formed mixed Pc components made the copolymers more complicated [217]. (iii) Polymerization of a Pc-attached monomer. In 2023, an AB_3-type Pc-containing monomer was obtained from the reaction of 4-((2,5,8,11-tetraoxatridecan-13-yl)oxy)phthalonitrile and 4-(4-hydroxyphenoxy) phthalonitrile and with the subsequent reaction with a tosylated oxanorbornene compound, enabling the generation of copolymers and homopolymers by ring opening metathesis polymerization. The photosensitizer properties in photodynamic inactivation efficacy against two bacteria were investigated due to the generation of reactive oxygen specues [218].

With the exception of the above Pc polymers, there is also another kind of polymer, namely Pc dendrimers. These dendrimers have large and controlled hyperbranched architecture, including an interior core or focal point, an interior branching unit, and a terminal moiety located in the outermost generation. The high generation number of branches makes the dendrimers into a 3D globular structure [219]. The first Pc dendrimer was introduced in 1997, possessing a zinc Pc core peripherally attached by poly(ether-amide) [220]. Generally, there are two methods to construct Pc dendrimers. One is the convergent approach, which was first explored in 1998,

generating a Pc-cored dendrimer from the cyclization of a poly(benzylether) dendritic phthalonitrile [221]. This method has been widely used to prepare various Pc dendrimers. In addition, there is a divergent strategy, which was established in 2004 for the construction of a Pc dendrimer bearing eight phosphorus dendritic substituents with the generation numbers up to eight [222]. There is also an interesting silicone Pc-based dendrimer, in which these dendritic moieties are grown from their axial positions from dichlorosilicone Pc reacting with a poly(benzyl ether) dendritic alcohol [223].

1.4.3.2 Phthalocyanine-Based COFs

Covalent organic frameworks (COFs) are a class of special porous organic polymers with well-defined periodic architectures [224]. They have been established since 2005 [225]. These crystalline materials can be prepared by engineering functional building blocks and linkages, exhibiting diverse applications such as gas storage and separation [226], sensing [227], catalysis [228], energy storage and conversion [229], and medicine [230]. In the early stages, reversible covalent linkages dominated the generation of ordered structures via a dynamic polymerization and error correction process [231]. This is also the same for Pc-based COFs. The first example was reported in 2010 [232]. Dichtel's group introduced a $BF_3.OEt_2$-catalyzed method to prepare crystalline boronate ester-linked Pc-based COFs, which were deduced from the solvothermal reaction between protected catechol-substituted metal-free Pc monomers and 1,4-phenylenebis(boronic acid) in mesitylene and 1,2-dichloroethane at 120 °C. This new COF displays an **sql** topological square lattice, exhibiting an eclipsed fashion to form 2.3 nm permanent porosity. In 2011, a nickel Pc-based COF was also prepared through the boronate esterification reaction of 2,3,9,10,16,17,23,24-octahydroxy-phthalocyaninato nickel(II) [$NiPc(OH)_8$] and 1,4-benzenediboronic acid in DMAc/o-dichlorobenzene, showing significantly enhanced yield of 90% in comparison with $BF_3.OEt_2$-catalyzed method (48%) [233] (Figure 1.20). These two methods, namely $BF_3.OEt_2$-catalyzed and catalyst-free approaches, have been used to form various boronate ester-linked Pc-based COFs based on various arylboronic acids reacting with catechol-protected and catechol-containing Pc monomers, respectively. However, this inherent reversibility of boronate ester-linked PC-based COFs leads to instability against solvents and chemicals, restraining further applications.

Until 2019, 2,3,9,10,16,17,23,24-octaaminophthalocyanine nickel(II) [$NiPc(NH_2)_8$] was used to condense with pyrene-4,5,9,10-tetraone, generating the stable phenazine-linked COF-DC-8 with a conductivity of $2.51 \times 10^{-3}\,S\,m^{-1}$. Interestingly, it has sensitive responses toward various redox-active gases, including NH_3, H_2S, NO, and NO_2 [234] (Figure 1.21a). The isostructural COFs have recorded device-relevant hole mobility and electrocatalytic activity for carbon dioxide reduction in water possibly due to the special conjugation structure [236, 237]. Three stable dioxin-linked PC-based COFs, CoPc-TFPN, have been constructed from the substitution of tetrafluorophthalonitrile (TFPN) with metallic 2,3,9,10,16,17,23,24-octahydroxyphthalocyanine ([$MPc(OH)_8$], M = Ni, Co, Zn) with the help of triethylamine (Et_3N) in *N*,*N*-DMA/mesitylene. NiPc/CoPc-TFPN COFs

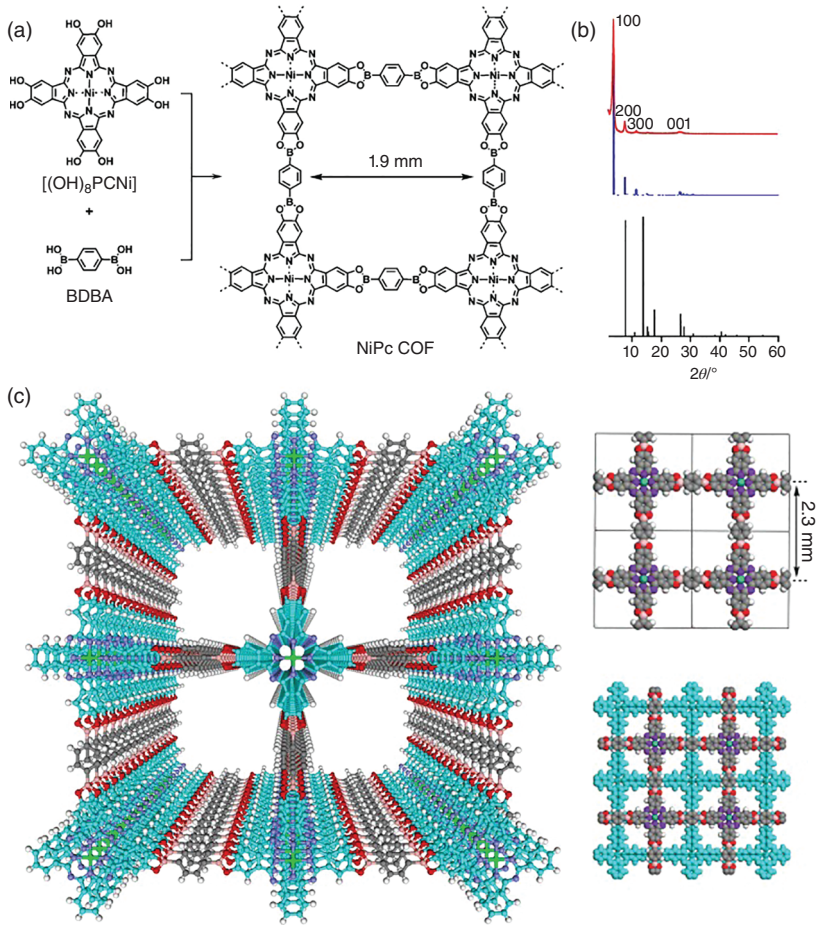

Figure 1.20 The synthesis of NiPc-COF by a boronate esterification reaction as well as PXRD patterns and structural models. Source: Reproduced from Ref. [233] / with permission of John Wiley & Sons.

have excellent electrocatalytic activity and selectivity toward CO_2 reduction under light irradiation [238]. With the exception of eight-substituted Pc monomer, the tetraanhydrides of 2,3,9,10,16,17,23,24-octacarboxyphthalocyanine were designed and prepared for constructing new COFs through the imidization reaction with rod-like aryldiamines in 2021 [239]. This kind of powerful building block was used for the preparation of robust 3D COFs by the imidization reaction with T_d-symmetric tetraamine [235] (Figure 1.21b).

The discovery of new synthesis methods and topological structures always attracts interest in the field of COFs. In 2021, a tetrahedral spiroborate linkage was applied to provide a 3D **nbo** topological COF with $[CoPc(OH)_8]$ as a building block [240]. The sp^3-hybridized nature of anionic boron center makes two Pc monomers in a perpendicular arrangement. The porous 3D COF shows excellent crystallinity and long-range order as indicated by the

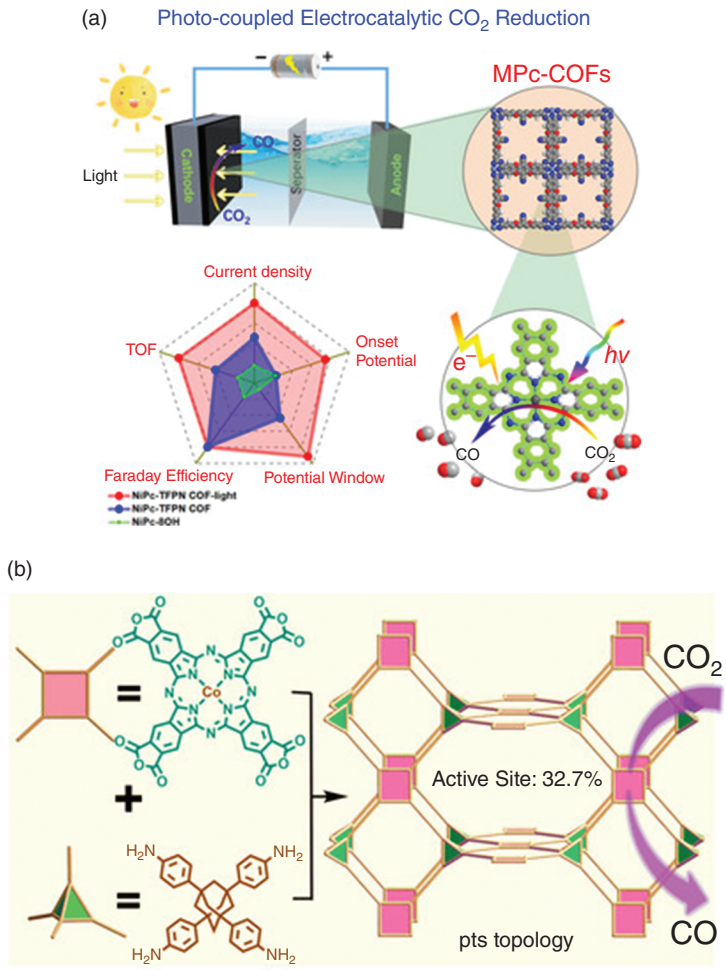

Figure 1.21 (a) Stable 2D Pc COFs Source: Adapted from Ref. [234]. and (b) 3D Pc COFs as electrocatalysts for CO_2 reduction. Source: Reproduced from Ref. [235] / with permission of John Wiley & Sons.

presence of 11 diffraction peaks in the PXRD pattern, allowing the observation of well-ordered crystal lattice using high-resolution transmission electron microscopy (HR-TEM). It has a high BET surface area of 1726 m^2 g^{-1}. At the same year, Zhang's group reported the nucleophilic aromatic substitution between copper(II) 1,2,3,4,8,9,10,11,15,16,17,18,22,23,24,25-hexadecafluoro-29H,31H-phthalocyanine [$CuPcF_{16}$] with cobalt(II) 2,3,9,10,16,17,23,24-octahydroxylphthalocyanine [$CoPc(OH)_8$] and cobalt(II) 3,4,12,13,21,22,30,31-octahydroxylnaphthalocyanine [$CoNPc(OH)_8$], generating robust bimetallic polyphthalocyanine COFs, CuPcF8-CoPc-COF and CuPcF8-CoNPc-COF, to resist harsh conditions. The electrocatalytic activities of these two COFs have been investigated toward CO_2 reduction reaction [241]. As can be seen from the above Pc-based COFs, they are all prepared

via solvothermal synthesis from Pc monomers as starting materials, requiring the long-time tedious synthesis of corresponding monomeric Pc compounds with different active sites. In 2022, Jiang's group introduced an ionothermal synthesis strategy to prepare Pc-based COFs. The polymerization of cyano group-containing Pc precursors, namely benzo[1,2-b,4,5-b′]bis[1,4]benzodioxin-2,3,9,10-tetracarbonitrile and quinoxalino[2′,3′,9,10]phenanthro[4,5-abc]phenazine-6,7,15,16-tetracarbonitrile, in $ZnCl_2$ at 350 °C for 8 hours afforded Pc-based COFs, namely BB-FACPc-COF and QPP-FAC-Pc-COF, respectively. Their crystallinity was comparable with their counterparts constructed by stepwise methods [242]. Various Pc-based COFs with modified monomers and different linkages have been reported. These researches will be introduced in the latter chapter.

1.5 Porous Polymeric Materials for Functional Applications

Although the synthesis of Pcs usually requires tedious and time-consuming procedures, their powerful functions attract intense interest in fabricating polymeric materials for the development of advanced non-noble metal catalysts, supracapacitors, sensors, battery electrodes, and so on. The porous structures are helpful in the diffusion of reagents and thus various applications. In addition, the planar conjugated Pc units are beneficial to electron conductivity and light response including absorption scope and specific excitonic effects. The various applications of polymeric materials have been briefly introduced in the following section.

1.5.1 Phthalocyanine-Based Polymeric Materials for Chemical Sensors

Chemiresistive gas sensors (CGSs) represent a new kind of gas-sensing technique, which have advantages such as low power, low cost, and high sensitivity to detect harmful gases. The operating principle involves observation of the changed conductivity of materials once they touch a testing gas. Nanoporous materials such as MOFs, COFs, and POPs have been demonstrated as outstanding candidates for CGSs because of their high specific surface area, rich open metal site, different functional groups, and conductive nature. They possess rapid response and good recovery times, remarkable selectivity, and sensitivity in checking gases. Due to the planar and conjugated nature of Pc organic monomers, 2D Pc-based MOFs have high conductivity and thus excellent chemiresistive gas-sensing property [243]. Meng et al. fabricated Pc-based 2D MOFs, NiPc-M (M = Ni and Cu), by using $[NiPc(OH)_8]$, to coordinate with Ni and Cu ions [244]. These 2D Pc-based MOFs are excellent candidates for chemiresistive gas sensing because they have highly dispersed active sites on the conductive layer. In particular, the good conductivity of 2D Pc-based MOFs ensures high sensitivity to the analyte gases (H_2S, NO, and NH_3). Furthermore, the replacement of MPc with metallonaphthalocyanine $[CoNPc(OH)_8]$ leads to the new 2D isoreticular MOFs, NiNPc-M, but with changed sensitivity and selectivity. These bimetallic MOFs have detection limits against

these gases at ppm and ppb levels upon low driving voltages (0.01–1.0 V). However, the response ($-\Delta G/G_0$) of both Cu-based MOFs, NiPc-Cu and NiNPc-Cu, is higher than that of Ni-based MOF sensors (NiPc-Ni and NiNPc-Ni, respectively) toward 40 ppm H_2S. For 1 ppm of NO, the latter two MOFs have better responses than the former two MOFs. Obviously, these Pc-ligand-based MOFs, NiPc-M, are 5.5 times higher than that of naphthalocyanine-based NiNPc-M. In 2022, heterobimetallic 2D conductive MOFs were designed based on the complexation of [$MPc(OH)_8$] (M = Co, Ni) with Cu nodes, displaying low-power chemiresistive sensing activity toward carbon monoxide (CO) (Figures 1.22a–d) [245]. Corresponding devices have a limit of detection (LOD) of 0.53–3.0 ppm at the driving voltage. The mechanism shows the important sensing role of Cu nodes to bind CO, and metallic Pc can tune and amplify the sensing signals. On the basis of the Pc-based MOF platform for CGSs, surface-hydrophobic modification was used for constructing polarity-selective chemiresistors in 2021 (Figures 1.22e–h) [246]. The film surface of Pc-based MOFs, Ni_2[$MPc(NH)_8$] (M = Cu or Ni), was grafted with aliphatic octadecyltrimethoxysilane (OTMS) for reducing its H_2O response but increasing the diffusion of volatile organic compounds (VOCs). Benefiting from the high conductivity and hydrophobic grafting, the sensing performance, in terms of response/recovery rate, for OTMS-modified Ni_2[$CuPc(NH)_8$], increased following the increase in proportion to polar gases because the much higher polarities provide gases with strong affinity with MOF active sites.

In contrast to Pc-based MOFs, their COF and polymer counterparts have been less used in the field of CGSs possibly due to the synthetic difficulty [247]. Although the intrinsic electrical conductivities of Pc-based COFs and polymers are moderate, their crystalline nature makes them as good candidates for electrochemical sensing though metal- and conductive carbon doping-based conductivity increments were reported previously. For example, stable phenazine-linked COF-DC-8 exhibits a conductivity of 2.51×10^{-3} S m^{-1}. It was directly dispersed onto interdigitated gold electrodes for their chemiresistive nature toward various gases with excellent results for NH_3, NO_2, H_2S, and NO gases [234]. In 2019, an electrochemical H_2O_2 sensor made up of diyne-linked iron Pc-conjugated polymeric NSs, FePc-CP NSs, was reported [248]. The exfoliation of FePc-CP NSs was achieved due to the presence of a defect and disorder structure in this conjugated polymer. FePc-CP NSs were made as multilayer films with controllable thickness on glass carbon electrodes using the quasi-Langmuir-Shafër method. They have good H_2O_2 sensing activity in the concentration scope of 0.1–1000 μM, a rapid response within 0.1 second, a high LOD of 0.017 μM, and a high sensitivity of 97 μA cm^{-2} mM^{-1}. The outstanding electrochemical H_2O_2 sensors are originated from the high density of active centers that are exposed on the electrode.

1.5.2 Phthalocyanine-Based Polymeric Materials for Electrocatalysis

The investigation of novel, efficient, and stable materials has always attracted intense attention in the field of electrochemical conversion. MPc-based molecular catalysts have demonstrated excellent heterogeneous electrocatalytic properties for

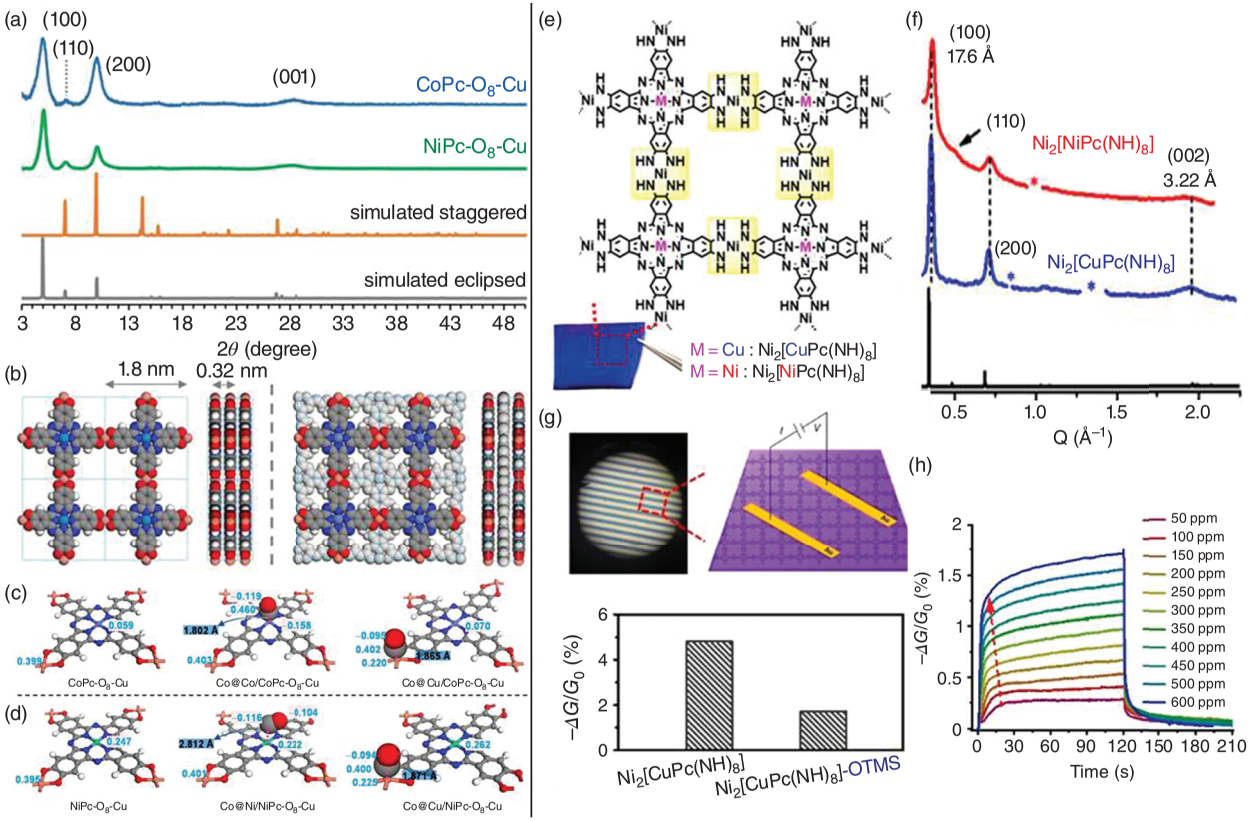

Figure 1.22 PXRD data, structure, and properties of MPc-O_8-Cu (a) Source: Reproduced from Ref. [245] / with permission of John Wiley & Sons. and $Ni_2[MPc(NH)_8]$ (b) (M = Co, Ni, Cu). Source: Reproduced from Ref. [246] / with permission of John Wiley & Sons.

energy conversion related to hydrogen, oxygen, water, carbon dioxide, and nitrogen. In particular, their well-defined M-N_4 (M = Fe, Co, Ni, Cu) microstructures and tailorable molecular advantages are beneficial to correlating the interrelationship between the electrocatalytic activity and structure and thus regulating the electronic configuration. The porous polymeric Pc-based materials are controlled from the level of atomic and molecular precision. In particular, those crystalline reticular materials, MOFs and COFs, have periodic structures to integrate versatile molecular units with the desired optoelectronic properties. MPc-based electrocatalysts have been employed as electrode materials in various electrochemical reactions, including hydrogen evolution reaction (HER), OER, oxygen reduction reaction (ORR), carbon dioxide reduction reaction (CO_2RR), and nitrogen reduction reaction (NRR). Before the electrocatalytic measurement, it is worth noting that the electrical conductivity of the materials plays an important role in the performance; these materials are usually used to make electrodes by doping a conductive carbon substrate. In addition, exfoliating the bulk 2D precursor enables the improvement of electrocatalytic activity [249–252].

ORR with either a direct or an indirect four-electron ($4e^-$) transport pathway is an important electron transfer process in the field of sustainable energy conversion systems. The high ORR performance is a result of electrochemical and electronic properties. Polymeric materials with MPc units have suitable metal redox potential, interaction strength between metal and oxygen intermediates, d-orbital electrons, and energy levels, serving as excellent candidates for ORR electrocatalysts. Generally, the hybrid materials composed of conjugated Pc-based polymers and conductive substrates (e.g. graphene, carbon nanotubes, and acetylene black) are made into electrodes. In 2019, three amorphous ethynyl-linked Pc polymers (MPc-CP, M = Fe, Co, $Fe_{0.5}Co_{0.5}$) were exfoliated into ultrathin NSs due to weakened interlayer interaction associated with the presence of intrinsic structural defects and a disordered nature for 2D framework [253]. The obtained MPc-CP NSs had a high yield of over 50% and possessed a uniform thickness of 1–3 nm and a size of hundreds of nanometers according to TEM and atomic force microscopy photographs. Especially, the heterometallic $Fe_{0.5}Co_{0.5}$Pc-CP NSs on graphene display excellent ORR activity, by means of an onset potential of 1.01 V and a half-wave potential of 0.93 V in 0.1 M KOH. Moreover, a Zn–air battery device was fabricated using this Pc-based electrocatalyst as a cathode, displaying an open circuit voltage of 1.34 V. In the field of ORR, conjugated metal polyphthalocyanines have been widely researched as electrochemical catalysts because the planar networks show full π-delocalization. For example, cobalt-containing polyphthalocyanine was functionalized at the framework edge with different aromatic acid anhydride substituents by ball milling [254]. The employment of tetraphenylphthalic anhydride results in the generation of uniform cobalt polyphthalocyanine (CoPPc)-p NSs with a thickness of 2.9 nm. Such material was fabricated into an electrode with excellent electrocatalytic ORR activity. Its smaller Tafel slope of 45 mV dec^{-1} indicates the high transfer coefficient in ORR kinetics. In particular, the mass activity is 44 mA $mg_{cat.}{}^{-1}$ at 0.9 V. This together with the stability is much more outstanding than the benchmark Pt/C catalyst. A primary Zn-air battery device was installed

utilizing CoPPc-p NSs as air electrode catalysts have superior performance to that of benchmark Pt/C catalyst.

In recent years, electrocatalysis of CO_2RR in water was revived due to the positive environmental and economic significance in the conversion of CO_2 into chemical fuels to reduce greenhouse gas emissions. CO_2RR is an endothermic process, and its mechanism is composed of (i) CO_2 binding with catalytically active sites, (ii) CO_2 activation and conversion through multi-electron/proton transfer process, and (iii) product desorption and configuration recovery. The first case of Pc-based polymeric material was reported in 2017. Li's group presented an organic–inorganic hybrid material by direct polymerization of cobalt polyphthalocyanine on carbon nanotubes for electrocatalysis of CO_2RR [255]. In comparison with the molecular catalyst, polyphthalocyanine manifests an improved electrochemically active surface area and cycling stability due to the robust hybrid structure. Especially, cobalt polyphthalocyanine shows highly selective conversion of CO_2 to CO with a high Faradaic efficiency of 90% in 0.5 M $NaHCO_3$, and the turnover frequency is accumulated to 4900 h^{-1} at an overpotential of 0.5 V. The reaction mechanism has been well understood using theoretical calculations. In 2020, a conjugated Pc-based COF, CoPc-PDQ-COF, with phenazine connection between 2,3,9,10,16,17,23,24-octakis(amino) Pc and 4,5,9,10-pyrenediquinone monomers, was attempted for electrocatalysis of CO_2RR [237]. The robust phenazine linkage provided the COF electrocatalyst with good cycling stability and conductivity due to the conjugation structure, leading to good catalytic activity and selectivity for CO_2 to CO conversion. In this direction, Pc-based MOFs have also been widely researched due to their high-density accessible metallic sites and good conductive characteristics. In addition to those 2D MOFs, conjugation polymers, and COFs, few 3D Pc-based cases, for example, CoPcMOF-1992, are also able to promote the conversion of CO_2 [179]. As a result, the rational engineering of modular architectures opens up a new avenue for electrocatalysis research based on these Pc-based polymeric materials.

1.5.3 Phthalocyanine-Based Polymeric Materials for Photocatalysts

Phthalocyanine-based polymeric materials have strong light absorption ability in the visible light region. This, in combination with the different active metal ions, provides the necessary requirement for various photocatalytic activities, including singlet oxygen generation, carbon dioxide conversion, and organic synthesis. Furthermore, the porous architecture is able to improve the transport of reagents and photogenerated carriers, achieving superior photocatalytic activity [256]. In 2015, Han et al. constructed a series of conjugated microporous polymers, MPc-CMPs (M = Co, Ni, Cu, Zn), through the imine condensation reaction of tetraaminometallophthalocyanine [$MPc(NH_2)_4$] and terephthalaldehyde (TA) in DMAc at 150 °C [257] (Figure 1.23). In comparison with molecular chromophores, porous MPc-CMP photosensitizers display stronger light-capturing capability in the long-wavelength region due to the extension of π-conjugation systems after imine connection. MPc-CMPs display high efficiency for photocatalytic $^1O_2$ synthesis

as indicated by 1,3-diphenylisobenzofuran as a singlet oxygen trapper. Among these porous polymers, ZnPc-CMP and CuPc-CMP have outstanding photocatalytic activity for singlet oxygen production under the irradiation of low energy light, demonstrating promising photosensitizer nature. At the same time, this group presents seven kinds of copper Pc-based polymers by the reaction of [$CuPc(NH_2)_4$] with either diamine or triamine linkers for photocatalytic singlet oxygen synthesis [258]. Wu *et al*. reported the 3D porous organic polymer CZJ-30, which was obtained from the iron tetraaminometallophthalocyanine [$FePc(NH_2)_4$] and 1,3,5-triformylbenzene (TFB). [259] A synergistic photocatalytic system made up of CZJ-30 and *N*-hydroxyphthalimide (NHPI) co-catalyst showed high conversion

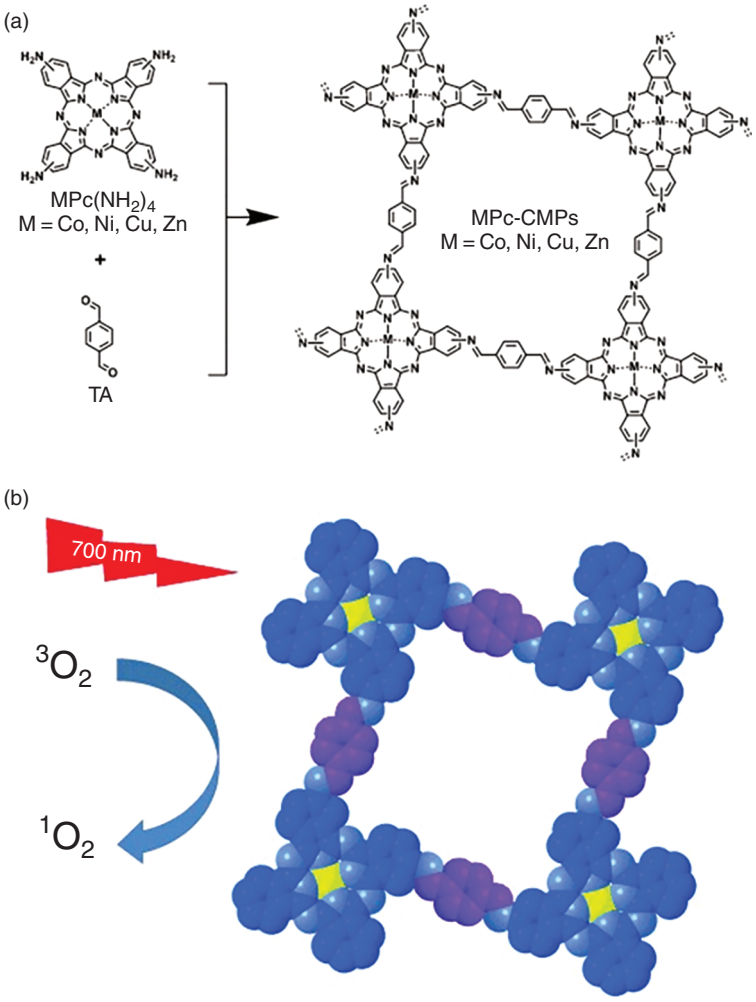

Figure 1.23 Synthesis of MPc-CMPs (CMPs: conjugated microporous polymers) for producing singlet oxygen. Source: Reproduced from Ref. [257] / with permission of John Wiley & Sons.

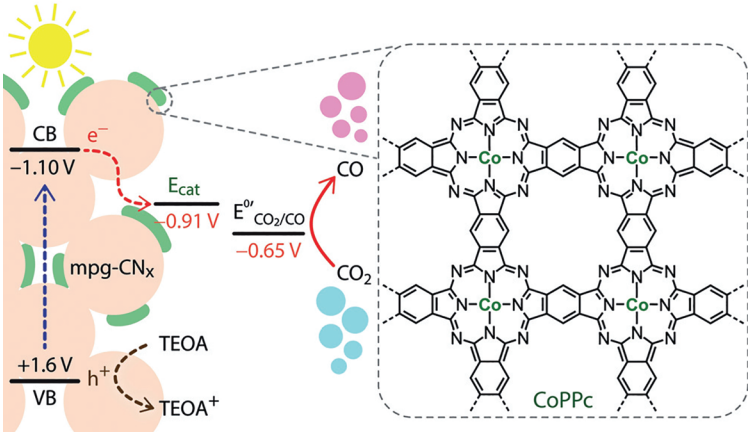

Figure 1.24 Schematic illustration of light-driven CO_2 reduction property and electronic structures of mpg-CN_x@CoPPc hybrid. Source: Ref. [260] / John Wiley & Sons / CC BY 4.0.

efficiency and recycling stability for the aerobic oxidation of arylalkanes. The conversion efficiency and selectivity of ethylbenzene were able to reach 95% and 99%, respectively. In 2019, a precious metal-free composite composed of CoPPc and mesoporous carbon nitride (mpg-CN_x) as the photosensitizer was assembled, selectively converting CO_2 to CO with a turnover number of 90 based on an active cobalt site after 60 hours (Figure 1.24) [260].

1.5.4 Phthalocyanine-Based Polymeric Materials for Energy Storage

The exploration of sustainable and safe alternative energy sources and storage devices is highly desirable in modern society. LIBs with higher energy and power densities have been widely used as recharged devices in daily life and industry. Their theoretical capacity was restricted by anode and cathode electrode materials, such as $LiFePO_4$ and graphite, respectively. In order to pursuit higher energy density, metal–air batteries (MABs) such as Li-O_2 and Zn-O_2 batteries were established to replace the intercalation mechanism in LIBs with the redox reaction between the metal and oxygen. For the development of such technologies, efficient and stable electrocatalysts are vital to accelerate the slow kinetics of redox reactions that occur at the electrode surface. MPcs constitute one kind of promising M-N_4-type molecular electrocatalysts with outstanding activity toward H_2, O_2, and CO_2 electrocatalysis. The electrocatalysis results of ORR and CO_2RR are briefly mentioned in the previous section. Now, the rechargeable Li-CO_2 battery technology upon polyphthalocyanine has been introduced as a representative of MAB. Instead of O_2, atmospheric CO_2 has been used as the energy carrier for this kind of MABs. Low-cost conjugated CoPPc has been demonstrated to exhibit good catalytic activity to reversibly form and decompose Li_2CO_3 [261]. CoPPc was obtained from the microwave heating reaction of 1,2,4,5-tetracyanobenzene and Co^{2+}. A *N*-methylpyrrolidone (NMP) suspension of CoPPc was deposited on a carbon

cloth to assemble Li-CO_2 battery. The good catalytic activity of CoPPc ensures the device with a high areal capacity of 13.6 mA h cm^{-2} and rate performances. In addition to the MABs, Pc-based polymeric materials have been used in different metal-ion batteries. For example, sodium-ion batteries (SIBs) have been proposed as a kind of next-generation energy storage device. Metallic polyphthalocyanines (MPPcs) due to the N-rich conjugation structure have been attempted as the SIBs' anode [262]. Molten salt reaction of tetracyanobenzene in the presence of $FeCl_2$, $Co(OAc)_2$, $Ni(OAc)_2$, and $Cu(OAc)_2$ at 350 °C under Ar generates MPPc (M = Fe, Co, Ni, and Cu). The coin-type cells fabricated by MPPc show high capacities up to 538 and 342 mA h g^{-1} at 50 and 1000 mA g^{-1}, respectively. In particular, their rate performance and cycling performances are similar to those of the excellent anode materials of SIBs.

1.6 Conclusion

In this chapter, we intend to summarize as much as contributions toward the construction of Pc-based functional polymeric materials mainly including coordination polymers and covalent organic polymers with well-defined structures, rather than those amorphous supramolecular nanostructural assemblies. In particular, we introduced the versatile chemistry from Pc-based monomer, oligomer, and polymeric materials including MOFs and COFs, making possible correlation between structures and functions at the basic and precise molecular levels. In addition, the preparation of functional monomeric macrocycles and the controlled organization of polymeric structures were presented. Finally, some examples of Pc-based polymeric materials were also displayed for their practical applications.

Abbreviations

AQ	Anthraquinone
ATRP	Atom transfer radical polymerization
BBTC	bBenzo[1,2-b:4,5-b′]bis[1,4]benzodioxin-2,3,9,10-tetracarbonitrile
BET	Brunauer–Emmett–Teller
C_{60}	Fullerene
CGSs	Chemiresistive gas sensors
CO_2RR	Carbon dioxide reduction reaction
COFs	Covalent–Organic Frameworks
D-A	Donor–Acceptacceptor
D-A-D	Donor–Acceptacceptor–Donordonor
DBU	1,8-diazabicyclo[5.4.0]undec-7-ene
DMA, DMAc	Dimethylacetamide
DMF	*N*,*N*-dimethylamino
DMSO	Dimethyl Sulfoxidesulfoxide
FE_{CO}	CO Faradaic efficiency

FTO	Fluorine-doped tin oxide
HMDS	Hexamethyl Disilazane
HOFs	Hydrogen-Bonded Organic Frameworks
HR-TEM	High -resolution transmission electron microscopy
IC_{50}	Inhibitory Concentration
M	Metal
MABs	Metal–Air Batteries
MOCs	Metal–Organic Cages
MOFs	Metal–Organic Frameworks
NHPI	*N*-hydroxyphthalimide
OFET	Organic Field Effect Transistor
ORR	Oxygen reduction reaction
OTMS	Octadecyltrimethoxysilane
Pcs	Phthalocyanines
PDIs	Perilendiimides
POCs	Porous Organic Cages
POSS	Silsesquioxanes
PVP	Polyvinylpyrrolidone
PXRD	Powder X-ray Diffractiondiffraction
QPPTC	quinoxalinoQuinoxalino[2′,3′:9,10]phenanthro[4,5-abc]phenazine-6,7,15,16-tetracarbonitrile
ROS	Reactive Oxygen Species
SBUs	Secondary Building Units
SCSC	Single crystal to single crystal
SCXRD	Single- Crystal X-ray Diffraction
SPB	Spiroborate
TA	Terephthalaldehyde
TCB	1,2,4-trichlorobenzene
TCNE	Tetracyanoethylene
$TEABF_4$	Tetraethylammonium Tetrafluoroborate
TFB	1,3,5-triformylbenzene
THF	Tetrahydrofuran
UV–vis	Ultraviolet–visible
VOCs	Volatile organic compounds

References

1 Ashby, M., Ferreira, P., and Schodek, D. (2009). *Nanomaterials, Nanotechnologies and Design*. Oxford: Butterworth-Heinemann Chapters. 1–5.
2 Desiraju, G.R. (2001). *Nature* 412: 397–400.
3 Lehn, J.M. (2017). *Chem. Soc. Rev.* 46: 2378–2379.
4 Amabilino, D.B. and Gale, P.A. (2017). *Chem. Soc. Rev.* 46: 2376–2377.
5 Global sustainable development report (2019). *The Future Is Now: Science for Achieving Sustainable Development*. New York: United Nations.

6 Li, H., Eddaoudi, M., O'Keeffe, M., and Yaghi, O.M. (1999). *Nature* 402: 276–279.
7 Côté, A.P., Benin, A.I., Ockwig, N.W. et al. (2005). *Science* 310: 1166.
8 Fujita, M., Oguro, D., Miyazawa, M. et al. (1995). *Nature* 378: 469–471.
9 Tozawa, T., Jones, J.T.A., Swamy, S.I. et al. (2009). *Nat. Mater.* 8: 973–978.
10 Wang, X., Simard, M., and Wuest, J.D. (1994). *J. Am. Chem. Soc.* 116: 12119–12120.
11 C. C. Leznoff, A. B. P. Lever, (1989, **1993**, **1996**) Phthalocyanines: properties and applications, vols 1–4. VCH Publishers, Cambridge.
12 McKeown, N.B. (1998). *Phthalocyanine materials: synthesis, structure and function*. Cambridge: Cambridge University Press.
13 Zhang, Y., Cai, X., Bian, Y., and Jiang, J. (2010). *Functional Phthalocyanine Molecular Materials* (ed. J. Jiang), 275–321. Berlin: Springer.
14 Byrne, G.T., Linstead, R.P., and Lowe, A.R. (1934). *J. Chem. Soc.* 1017–1022.
15 Linstead, R.P. and Lowe, A.R. (1934). *J. Chem. Soc.* 1022–1027.
16 Dent, C.E. and Linstead, R.P. (1934). *J. Chem. Soc.* 1027–1031.
17 Dent, C.E., Linstead, R.P., and Lowe, A.R. (1934). *J. Chem. Soc.* 1033–1039.
18 Robertson, J.M. (1935). *J. Chem. Soc.* 615–621.
19 Robertson, J.M. (1936). *J. Chem. Soc.* 1195–1209.
20 Robertson, J.M. and Woodward, I. (1937). *J. Chem. Soc.* 219–230.
21 de la Torre, G., Vazquez, P., Agullo-Lopez, F., and Torres, T. (2004). *Chem Rev.* 104: 3723–3750.
22 Jiang, J. and Ng, D.K.P. (2009). *Acc. Chem. Res.* 42: 79–88.
23 de la Torre, G., Bottari, G., Sekita, M. et al. (2013). *Chem. Soc. Rev.* 42: 8049–8105.
24 Yang, B., Chen, Y., and Shi, J. (2019). *Chem. Rev.* 119: 4881–4985.
25 Singh, S., Aggarwal, A., Bhupathiraju, N.V.S.D.K. et al. (2015). *Chem. Rev.* 115: 10261–10306.
26 Li, X., Park, E.-Y., Kang, Y. et al. (2020). *Angew. Chem. Int. Ed.* 59: 8630–8634.
27 Alzeer, J., Vummidi, B., Roth, P., and Luedtke, N.W. (2009). *Angew. Chem. Int. Ed.* 48: 9362–9365.
28 Perovic, A. (1987). *J. Matei. Sci.* 22: 835–838.
29 Schwarze, M., Tress, W., Beyer, B. et al. (2016). *Science* 352: 1446–1449.
30 Wu, W.T., Chen, X., Jiao, Y.T. et al. (2022). *Angew. Chem. Int. Ed.* 61: e202115820.
31 Leclaire, J., Dagiral, R., Fery-Forgues, S. et al. (2005). *J. Am. Chem. Soc.* 127: 15762–15770.
32 Miyoshi, Y., Kubo, M., Fujinawa, T. et al. (2007). *Angew. Chem. Int. Ed.* 46: 5532–5536.
33 Alcón, I., Gonidec, M., Ajayakumar, M.R. et al. (2016). *Chem. Sci.* 7: 4940–4944.
34 Warner, M., Din, S., Tupitsyn, I.S. et al. (2013). *Nature* 503: 504–508.
35 Drobizhev, M., Makarov, N.S., Rebane, A. et al. (2006). *H. Proc. SPIE* 6308: 630803.
36 Gonidec, M., Luis, F., Vílchez, J.E. et al. (2010). *Angew. Chem. Int. Ed.* 49: 1623–1626.

37 Chang, B., Lee, H., Kwon, Y. et al. (2010). *Adv. Mater.* 751: 4405–4409.
38 Jailaubekov, A.E., Willard, A.P., Tritsch, J.R. et al. (2013). *Nat. Mater.* 12: 66–73.
39 Hu, Q., Rezaee, E., Xu, W. et al. (2021). *Small* 17: 2005216.
40 Han, B., Ding, X., Yu, B. et al. (2021). *J. Am. Chem. Soc.* 143: 7104–7113.
41 Han, B., Jin, Y., Chen, B. et al. (2022). *Angew. Chem. Int. Ed.* 61: e202114244.
42 Han, B., Liang, B., Zhang, E. et al. (2024). *Adv. Funct. Mater.* 2404289.
43 O'Flaherty, S.M., Hold, S.V., Cook, M.J. et al. (2003). *Adv. Mater.* 15: 19–32.
44 Hanack, M., Schneider, T., Barthel, M. et al. (2001). *Coord. Chem. Rev.* 219–221: 235–258.
45 Lu, M., Zhang, M., Liu, C.-G. et al. (2021). *Angew. Chem. Int. Ed.* 60: 4864–4871.
46 Wang, X., Bahri, M., Fu, Z. et al. (2021). *J. Am. Chem. Soc.* 143: 15011–15016.
47 Zhang, P., Wang, M., Liu, Y. et al. (2023). *J. Am. Chem. Soc.* 145: 6247–6256.
48 Lo, P.-C., Leng, X., and Ng, D.K.P. (2007). *Chem. Rev.* 251: 2334–2353.
49 Bottari, G., Olea, D., Gómez-Navarro, C. et al. (2008). *Angew. Chem. Int. Ed.* 47: 2026–2031.
50 Furuyama, T., Sato, T., and Kobayashi, N. (2015). *J. Am. Chem. Soc.* 137: 13788–13791.
51 Yoshimoto, S., Honda, Y., Ito, O., and Itaya, K. (2008). *J. Am. Chem. Soc.* 130: 1085–1092.
52 Liu, J., Chen, T., Deng, X. et al. (2011). *J. Am. Chem. Soc.* 133: 21010–21015.
53 Urdampilleta, M., Klyatskaya, S., Cleuziou, J.P. et al. (2011). *Nat. Mater.* 10: 502–506.
54 McKeown, N.B. (2003). Phthalocyanines. In: *Comprehensive Coordination Chemistry*, 2nde, vol. 1, 507–514. Amsterdam: Elsevier and references therein.
55 Kopylovich, M.N., Kukushkin, V.Y., Haukka, M. et al. (2004). *J. Am. Chem. Soc.* 126: 15040–15041.
56 Langerreiter, D., Kostiainen, M.A., Kaabel, S., and Anaya-Plaza, E. (2022). *Angew. Chem. Int. Ed.* 61: e202209033.
57 Achar, B.N., Fohlen, G.M., Parker, J.A., and Keshavayya, J. (1987). *Polyhedron* 6: 1463–1467.
58 Wöhrle, D., Buck, T., Hündorf, U. et al. (1989). *Makromol. Chem.* 190: 961–974.
59 Zhong, T., Ding, L., and Long, L. (2001). *Hechenghuaxue* 9: 534–536. https://doi.org/10.3969/j.issn.1005-1511.2001.06.015.
60 Ali, H., Cauchon, N., and van Lier, J.E. (2009). *Photochem. Photobiol. Sci.* 8: 868–874.
61 Kimura, M., Hamakawa, T., Hanabusa, K. et al. (2001). *Inorg. Chem.* 40: 4775–4779.
62 Chen, J., Zhang, Q., Zeng, M. et al. (2016). *J. Solid State Electrochem.* 20: 1285–1294.
63 Namgoong, J.W., Kim, H.M., Kim, S.H. et al. (2021). *Dyes Pigm.* 184: 108737.
64 Gorduk, S. (2021). *J. Organomet. Chem.* 936: 121707.
65 Yuksel, F., Gurek, A.G., Lebrun, C., and Ahsen, V. (2005). *New J. Chem.* 29: 726–732.

66 Yuksel, F., Tuncel, S., and Ahsen, V. (2008). *J. Porphyrins Phthalocyanines* 12: 123–130.

67 Chen, Y., Liu, C., Ma, F. et al. (2018). *Chem. A Eur. J.* 24: 8066–8070.

68 Ng, D.K.P. and Jiang, J. (1997). *Chem. Soc. Rev.* 26: 433–442.

69 Barrett, P.A., Dent, C.E., and Linstead, R.P. (1936). *J. Chem. Soc.* 1719–1736.

70 Kirin, I.S., Moskalev, P.N., and Makashev, Y.A. (1965). *Russ. J. Inorg. Chem.* 10: 1065–1066.

71 Kasuga, K., Tsutsui, M., Petterson, R.C. et al. (1980). *J. Am. Chem. Soc.* 102: 4835–4836.

72 Kasuga, K., Ando, M., Morimoto, H., and Isa, M. (1986). *Chem. Lett.* 15: 1095–1098.

73 Martynov, A.G., Horii, Y., Katoh, K. et al. (2022). *Chem. Soc. Rev.* 51: 9262–9339.

74 Wang, H., Wang, B.-W., Bian, Y. et al. (2016). *Coord. Chem. Rev.* 306: 195–216.

75 De Cian, A., Moussavi, M., Fischer, J., and Weiss, R. (1985). *Inorg. Chem.* 24: 3162–3167.

76 Pushkarev, V.E., Tomilova, L.G., and Nemykin, V.N. (2016). *Coord. Chem. Rev.* 319: 110–179.

77 Wang, H., Qian, K., Wang, K. et al. (2011). *Chem. Commun.* 47: 9624–9626.

78 Fukuda, T., Biyajima, T., and Kobayashi, N. (2010). *J. Am. Chem. Soc.* 132: 6278–6279.

79 Liu, C., Yang, W., Zhang, Y., and Jiang, J. (2020). *Inorg. Chem.* 59: 17591–17599.

80 Wang, H., Qi, D., Xie, Z. et al. (2013). *Chem. Commun.* 49: 889–891.

81 Liu, Y., Shigehara, K., Hara, M., and Yamada, A. (1991). *J. Am. Chem. Soc.* 113: 440–443.

82 Horii, Y., Katoh, K., Breedlove, B.K., and Yamashita, M. (2017). *Chem. Commun.* 53: 8561–8564.

83 Horii, Y., Kishiue, S., Damjanović, M. et al. (2018). *Chem. Eur. J.* 24: 4320–4327.

84 Zhang, H., Wang, R., Zhu, P. et al. (2004). *Inorg. Chem.* 43: 4740–4742.

85 Liu, C., Yang, W., Wang, J. et al. (2021). *Dalton Trans.* 50: 13661–13665.

86 Moussavi, M., De Cian, A., Fischer, J., and Weiss, R. (1986). *Inorg. Chem.* 25: 2107–2108.

87 Chabach, D., De Cian, A., Fischer, J. et al. (1996). *Angew. Chem., Int. Ed. Engl.* 35: 898–899.

88 Chabach, D., Tahiri, M., De Cian, A. et al. (1995). *J. Am. Chem. Soc.* 117: 8548–8556.

89 Gonidec, M., Davies, E.S., McMaster, J. et al. (2010). *J. Am. Chem. Soc.* 132: 1756–1757.

90 Wang, H., Wang, K., Tao, J., and Jiang, J. (2012). *Chem. Commun.* 48: 2973–2975.

91 Birin, K.P., Gorbunova, Y.G., and Tsivadze, A.Y. (2012). *Dalton Trans.* 41: 9672–9681.

92 Wang, H., Wang, K., Bian, Y. et al. (2011). *Chem. Commun.* 47: 6879–6881.

93 Lu, G., He, C., Fang, Y. et al. (2018). *New J. Chem.* 42: 2498–2503.

94 Zhang, Y., Cao, W., Wang, K., and Jiang, J. (2014). *Dalton Trans.* 43: 9152–9157.

95 Liu, W., Zeng, S., Chen, X. et al. (2018). *Inorg. Chem.* 57: 12347–12353.
96 Cui, L., Zhu, F., Leong, C.F. et al. (2015). *Sci. China: Chem.* 58: 650–657.
97 Zhang, D., Wang, H., Chen, Y. et al. (2009). *Dalton Trans.* 9418–9425.
98 Ohashi, M., Konkol, M., Rosal, I.D. et al. (2008). *J. Am. Chem. Soc.* 130: 6920–6921.
99 Sorokin, A.B. (2019). *Coord. Chem. Rev.* 389: 141–160.
100 Das, S.K., Kc, C.B., Ohkubo, K. et al. (2013). *Chem. Commun.* 49: 2013–2015.
101 Cammidge, A.N., Nekelson, F., Hughes, D.L. et al. (2010). *J. Porphyrins Phthalocyanines* 14: 1001–1011.
102 Ercolani, C., Gardini, M., Monacelli, F. et al. (1983). *Inorg. Chem.* 22: 2584–2589.
103 Sorokin, A.B. and Tuel, A. (1999). *New J. Chem.* 23: 473–476.
104 Sorokin, A.B. (2017). *Adv. Inorg. Chem.* 70: 107–165.
105 Cammidge, A.N., Nekelson, F., Helliwell, M. et al. (2005). *J. Am. Chem. Soc.* 127: 16382–16383.
106 Zhao, Z., Cammidge, A.N., Hughes, D.L., and Cook, M.J. (2010). *Org. Lett.* 12: 5138–5141.
107 Afanasiev, P. and Sorokin, A.B. (2016). *Acc. Chem. Res.* 49: 583–593.
108 Bakshi, E.N., Delfs, C.D., Murray, K.S. et al. (1988). *Inorg. Chem.* 27: 4318–4320.
109 Cook, M.J. and Jafari-Fini, A. (1997). *J. Mater. Chem.* 7: 2327–2329.
110 Ishii, K., Abiko, S., Fujitsuka, M. et al. (1735–1739). *J. Chem. Soc. Dalton Trans.* 2002.
111 Ishii, K., Iwasaki, M., and Kobayashi, N. (2007). *Chem. Phys. Lett.* 436: 94–98.
112 Kameyama, K., Morisue, M., Satake, A., and Kobuke, Y. (2005). *Angew. Chem. Int. Ed.* 44: 4763–4766.
113 Kobayashi, N. and Muranaka, A. (1855–1856). *Chem. Commun.* 2000.
114 Rodríguez-Morgade, M.S., Plonska-Brzezinska, M.E., Athans, A.J. et al. (2009). *J. Am. Chem. Soc.* 131: 10484–10496.
115 Fernandez-Ariza, J., Krick-Calderon, R.M., Rodriguez-Morgade, M.S. et al. (2016). *J. Am. Chem. Soc.* 138: 12963–12974.
116 Trukhina, O., Rudolf, M., Bottari, G. et al. (2015). *J. Am. Chem. Soc.* 137: 12914–12922.
117 García-Iglesias, M., Peuntinger, K., Kahnt, A. et al. (2013). *J. Am. Chem. Soc.* 135: 19311–19318.
118 D'Souza, F., Maligaspe, E., Ohkubo, K. et al. (2009). *J. Am. Chem. Soc.* 131: 8787–8797.
119 D, Souza, F., Maligaspe, E., Sandanayaka, A.S.D. et al. (2010). *J. Phys. Chem. A* 114: 10951–10959.
120 Seitz, W., Jiménez, A.J., Carbonell, E. et al. (2010). *Chem. Commun.* 46: 127–129.
121 Leznoff, C.C., Lam, H., Marcuccio, S.M. et al. (1987). *J. Chem. Soc., Chem. Commun* 699–701.
122 Yang, J. and van de Mark, M.R. (1993). *Tetrahedron Lett.* 34: 5223–5226.
123 Dubinina, T.V., Ivanov, A.V., Borisova, N.E. et al. (2010). *Inorg. Chim. Acta* 363: 1869–1878.

124 Trashin, S.A., Dubinina, T.V., Fionov, A.V., and Tomilova, L.G. (2011). *J. Porphyrins Phthalocyanines* 15: 1195–1201.

125 Wang, K., Qi, D., Wang, H. et al. (2013). *Chem. Eur. J.* 19: 11162–11166.

126 Makarov, S.G., Piskunov, A.V., Suvorova, O.N. et al. (2007). *Chem. Eur. J.* 13: 3227–3233.

127 Pan, H., Li, S., Kan, J.-l. et al. (2019). *Chem. Sci.* 10: 8246–8252.

128 Wang, K., Qi, D., Mack, J. et al. (2012). *Chin. J. Inorg. Chem.* 28: 1779–1789.

129 Zhang, Y., Xue, Z., Qi, D. et al. (2017). *Chem. Eur. J.* 23: 15017–15021.

130 Zhang, Y., Oh, J., Wang, K. et al. (2016). *Chem. Eur. J.* 22: 4492–4499.

131 Zhang, Y., Zhao, L., Wang, K., and Jiang, J. (2017). *Inorg. Chem. Front.* 4: 104–109.

132 Wang, K., Huang, C., Pan, H. et al. (2017). *Inorg. Chem. Front.* 4: 110–113.

133 Shang, H., Xue, Z., Wang, K. et al. (2017). *Chem. Eur. J.* 23: 8644–8651.

134 Follana-Berná, J., Seetharaman, S., Martin-Gomiz, L. et al. (2018). *Phys. Chem. Chem. Phys.* 20: 7798–7807.

135 Vigh, S., Lam, H., Janda, P. et al. (1991). *Can. J. Chem.* 69: 1457–1461.

136 Bottari, G. and Torres, T. (2004). *Chem. Commun.* 2668–2669.

137 Cook, M.J. and Heeney, M.J. (2000). *Chem. Eur. J.* 6: 3958–3967.

138 García-Frutos, E.M., Ferneández-Lázaro, F., Maya, E.M. et al. (2000). *J. Org. Chem.* 65: 6841–6846.

139 Fukuda, T., Masuda, S., and Kobayashi, N. (2007). *J. Am. Chem. Soc.* 129: 5472–5479.

140 Gouloumis, A., González-Rodríguez, D., Vázquez, P. et al. (2006). *J. Am. Chem. Soc.* 128: 12674–12684.

141 Li, X., Sinks, L.E., Rybtchinski, B., and Wasilewski, M.R. (2004). *J. Am. Chem. Soc.* 126: 10810–10811.

142 García-Iglesias, M., Torres, T., and González-Rodríguez, D. (2016). *Chem. Commun.* 52: 9446–9449.

143 de la Torre, G., Bottari, G., Sekita, M. et al. (2013). *Chem. Soc. Rev.* 42: 8049–8105.

144 Isago, H., Terekhov, D., and Leznoff, C.C. (1997). *J. Porphyrins Phthalocyanines* 1: 135–140.

145 Leznoff, C.C., Lam, H., Nevin, W.A. et al. (1987). *Angew. Chem. Int. Ed. Engl.* 26: 1021–1023.

146 O'Malley, S., Schazmann, B., Diamond, D., and Nolan, K. (2007). *Tetrahedron Lett.* 48: 9003–9007.

147 Tolbin, A.Y., Ivanov, A.V., Tomilova, L.G., and Zefirov, N.S. (2003). *J. Porphyr. Phthalocyanines* 7: 162–166.

148 Bekaroğlu, Ö. (2010). *Functional Phthalocyanine Molecular Materials*, vol. 135 (ed. J. Jiang), 105–136. Berlin: Springer.

149 Erzunov, D., Tikhomirova, T., Botnar, A. et al. (2019). *Mini. Rev. Org. Chem.* 16: 410–421.

150 Tolbin, A.Y., Ivanov, A.V., Tomilova, L.G., and Zefirov, N.S. (2002). *Mendeleev Commun.* 96–97.

151 Ceyhan, T., Altindal, A., Özkaya, A.R. et al. (2007). *J. Porphyrins Phthalocyanines* 11: 625.
152 Yazıcı, A., Dalbul, N., Altındal, A. et al. (2016). *Synth. Met.* 212: 25–30.
153 Koçyiğit, N., Özen, Ü.E., Özer, M. et al. (2017). *Electrochim. Acta.* 233: 237–248.
154 Ceyhan, T., Altındal, A., Özkaya, A.R. et al. (2009). *Dalton Trans.* 10318–10329.
155 Özer, M., Altindal, A., Özkaya, A.R., and Bekaroğlu, Ö. (2009). *Dalton Trans.* 3175–3181.
156 Ali Özdağ, M., Ceyhan, T., Ünver, H. et al. (2010). *Opt. Commun.* 283: 330–334.
157 Yabaş, E., Bağda, E., and Bağda, E. (2015). *Dyes. Pigm.* 120: 220–227.
158 Fazio, E., Haynes, C.J.E., de la Torre, G. et al. (2018). *Chem. Commun.* 54: 2651–2654.
159 Salazar, A., Moreno-Simoni, M., Kumar, S. et al. (2023). *Angew. Chem. Int. Ed.* 62: e202311255.
160 Hu, Y.M., Huang, S.D., Wayment, L.J. et al. (2023). 101285. *Cell Rep Phys Sci* 4.
161 McKeown, N.B., Makhseed, S., Msayib, K.J. et al. (2005). *Angew. Chem. Int. Ed* 44: 7546–7549.
162 Makhseed, S., Ibrahim, F., Samuel, J. et al. (2008). *Chem. Eur. J.* 14: 4810–4815.
163 Bezzu, C.G., Helliwell, M., Warren, J.E. et al. (2010). *Science* 327: 1627–1630.
164 Bezzu, C.G., Burt, L.A., McMonagle, C.J. et al. (2019). *Nat. Mater.* 18: 740–745.
165 Wang, C., Wang, H., Liu, C. et al. (2019). *Inorg. Chem. Front* 6: 654–658.
166 Wang, C., Qi, D., Lu, G. et al. (2019). *Inorg. Chem. Front.* 6: 3345–3349.
167 Wang, H., Qian, K., Qi, D. et al. (2014). *Chem. Sci.* 5: 3214–3220.
168 Katoh, K., Yasuda, N., Damjanović, M. et al. (2020). *Chem. Eur. J.* 26: 4805–4815.
169 Kojima, T., Honda, T., Ohkubo, K. et al. (2008). *Angew. Chem. Int. Ed.* 47: 6712–6716.
170 Furukawa, H., Cordova, K.E., O'Keeffe, M., and Yaghi, O.M. (2013). 1230444. *Science* 341.
171 Li, B., Wen, H.M., Cui, Y. et al. (2016). *Adv. Mater.* 28: 8819–8860.
172 Litvinov, A.L., Kuzmin, A.V., Yudanova, E.I. et al. (2016). *Eur. J. Inorg. Chem.* 5445–5448. https://doi.org/10.1002/ejic.201600944.
173 Stone, K.H., Stephens, P.W., Wainer, M.B. et al. (2015). *Inorg. Chim. Acta.* 424: 116–119.
174 Abrahams, B.F., Hoskins, B.F., and Michail, D.M. (1994). R. Robson. *Nature* 369: 727–729.
175 Abrahams, B.F., Hoskins, B.F., and Robson, R. (1991). *J. Am. Chem. Soc.* 113: 3606–3607.
176 Lin, K.-J. (1999). *Angew. Chem., Int. Ed.* 38: 2730–2732.
177 Gao, W.-Y., Chrzanowski, M., and Ma, S. (2014). *Chem. Soc. Rev.* 43: 5841–5866.
178 Jia, H., Yao, Y., Zhao, J. et al. (2018). *J. Mater. Chem. A* 6: 1188–1195.
179 Matheu, R., Gutierrez-Puebla, E., Monge, M.Á. et al. (2019). *J. Am. Chem. Soc.* 141: 17081–17085.
180 Qiao, G.Y., Yuan, S., Pang, J.D. et al. (2020). *Angew. Chem. Int. Ed.* 59: 18224–18228.

181 Li, X., Rajasree, S.S., Gude, V. et al. (2023). *Angew. Chem. Int. Ed.* 62: e202219046.
182 Luo, T., Nash, G.T., Xu, Z. et al. (2021). *J. Am. Chem. Soc.* 143: 13519–13524.
183 Nash, G.T., Luo, T., Lan, G. et al. (2021). *J. Am. Chem. Soc.* 143: 2194–2199.
184 Yang, H., Yang, D., Zhou, Y., and Wang, X. (2021). *J. Am. Chem. Soc.* 143: 13721–13730.
185 Chen, X., Geng, K., Liu, R. et al. (2020). *Angew. Chem., Int. Ed.* 59: 5050–5091.
186 Martínez-Abadía, M. and Mateo-Alonso, A. (2020). *Adv. Mater.* 32: 2002366.
187 Waller, P.J., Gándara, F., and Yaghi, O.M. (2015). *Acc. Chem. Res.* 48: 3053–3063.
188 El-Kaderi, H.M., Hunt, J.R., Mendoza-Cortés, J.L. et al. (2007). *Science* 316: 268–272.
189 Yaghi, O.M. (2016). *J. Am. Chem. Soc.* 138: 15507–15509.
190 Diercks, C.S. and Yaghi, O.M. (2017). *Science* 355: eaal1585.
191 McKeown, N.B. and Budd, P.M. (2006). *Chem. Soc. Rev.* 35: 675–683.
192 A. Bucher, U. S. Patent 2,492,732 (1949)
193 Sprague Electric Co (1952). Final Report under contract No. D.A.-36-039-SC-87 to the United States Signal Corps, May 14 through October 15, 1952; ASTIA AD No. 6116.
194 W. C. Drinkard 1956. Ph.D. Thesis under Professor J. C, Bailar, University of Illinois.
195 Marvel, C.S. and Martin, M.M. (1958). *J. Am. Chem. Soc.* 80: 6600–6604.
196 Marvel, C.S. and Rassweiler, J.H. (1958). *J. Am. Chem. Soc.* 80: 1197–1199.
197 Snow, A.W., Griffith, J.R., and Marullo, N.P. (1984). *Macromolecules* 17: 1614–1624.
198 Ahsen, V., Yilmazer, E., and Bekâroğlu, Ö. (1988). *Makromol. Chem.* 189: 2533–2543.
199 Ahsen, V., Yilmazer, E., Gül, A., and Bekâroğlu, Ö. (1987). *Makromol. Chem., Rapid Commun.* 8: 243–246.
200 McKeown, N.B. (2000). *J. Mater. Chem.* 10: 1979–1995.
201 Wohrle, D. and Schulte, B. (1988). *Makromol. Chem.* 189: 1229–1238.
202 McKeown, N.B., Makhseed, S., and Budd, P.M. (2002). *Chem. Commun.* 23: 2780–2781.
203 Hashem, M., Bezzu, C.G., Kariuki, B.M., and McKeown, N.B. (2011). *Polym. Chem.* 2: 2190–2192.
204 Epstein, A. and Wildi, B.S. (1960). *J. Chem. Phys.* 32: 324–329.
205 Abel, M., Clair, S., Ourdjini, O. et al. (2011). *J. Am. Chem. Soc.* 133: 1203–1205.
206 Gomez-Romero, P., Lee, Y.S., and Kertesz, M. (1988). *Inorg. Chem.* 27: 3672–3675.
207 Honda, Z., Sakaguchi, Y., Tashiro, M. et al. (2017). *Appl. Phys. Lett.* 110: 133101.
208 Wang, X., Sun, S., Yao, J. et al. (2024). *Energy Environ. Mater.* 0: e12709.
209 Bryant, G.C., Cook, M.J., Ryan, T.G., and Thorne, A.J. (1995). *J. Chem. Soc., Chem. Commun.* 467–468.
210 Chen, W., Liu, F., Lü, W. et al. (2008). *Sci China Ser B-Chem* 51: 570–576.
211 Joyner, R.D. and Kenney, M.E. (1960). *J. Am. Chem. Soc.* 82: 5790–5791.

212 Dirk, C.W., Inabe, T., Schoch, K.F. Jr., and Marks, T.J. (1983). *J. Am. Chem. Soc.* 105: 1539–1550.
213 Hanack, M. and Lang, M. (1994). *Adv. Mater.* 6: 819–833.
214 Marks, T.J. (1985). *Science* 227: 881–889.
215 McKeown, N.B. (2000). *J. Mater. Chem.* 10: 1979–1995.
216 Aimi, J., Komura, M., Iyoda, T. et al. (2015). *J. Mater. Chem. C* 3: 2484–2490.
217 Jeong, J., Lee, Y.-J., Kim, B. et al. (2015). *Polym. Chem.* 6: 3392–3397.
218 Ahmetali, E., Galstyan, A., Süer, N.C. et al. (2023). *Polym. Chem.* 14: 259–267.
219 Li, W.-S. and Aida, T. (2009). *Chem. Rev.* 109: 6047–6076.
220 Kimura, M., Nakada, K., Yamaguchi, Y. et al. (1997). *Chem. Commun.* 1215–1216.
221 Brewis, M. and Clarkson, G.J. (1998). *Chem. Commun.* 969–970.
222 Leclaire, J., Coppel, Y., Caminade, A.M., and Majoral, J.P. (2004). *J. Am. Chem. Soc.* 126: 2304–2305.
223 Brewis, M., Clarkson, G.J., Goddard, V. et al. (1998). *Angew. Chem. Int. Ed.* 37: 1092–1094.
224 Diercks, C.S. and Yaghi, O.M. (2017). *Science* 355: eaal1585.
225 Ding, S.-Y. and Wang, W. (2013). *Chem. Soc. Rev.* 42: 548–568.
226 Dou, H., Xu, M., Wang, B. et al. (2021). *Chem. Soc. Rev.* 50: 986–1029.
227 Liu, X., Huang, D., Lai, C. et al. (2019). *Chem. Soc. Rev.* 48: 5266–5302.
228 Basak, A., Karak, S., and Banerjee, R. (2023). *J. Am. Chem. Soc.* 145: 7592–7599.
229 Liu, X., Jin, Y., Wang, H. et al. (2022). *Adv. Mater.* 34: 2203605.
230 Kim, J.H., Kang, D.W., Yun, H. et al. (2022). *Chem. Soc. Rev.* 51: 43–56.
231 Jin, Y., Yu, C., Denman, R.J., and Zhang, W. (2013). *Chem. Soc. Rev.* 42: 6634–6654.
232 Spitler, E.L. and Dichtel, W.R. (2010). *Nat. Chem.* 2: 672–677.
233 Ding, X., Guo, J., Feng, X. et al. (2011). *Angew. Chem. Int. Ed.* 50: 1289–1293.
234 Meng, Z., Stolz, R.M., and Mirica, K.A. (2019). *J. Am. Chem. Soc.* 141: 11929–11937.
235 Han, B., Jin, Y., Chen, B. et al. (2022). *Angew. Chem. Int. Ed.* 61: e202114244.
236 Wang, M., Ballabio, M., Wang, M. et al. (2019). *J. Am. Chem. Soc.* 141: 16810–16816.
237 Huang, N., Lee, K.H., Yue, Y. et al. (2020). *Angew. Chem. Int. Ed.* 59: 16587–16593.
238 Lu, M., Zhang, M., Liu, C.-G. et al. (2021). *Angew. Chem. Int. Ed.* 60: 4864–4871.
239 Han, B., Ding, X., Yu, B. et al. (2021). *J. Am. Chem. Soc.* 143: 7104–7113.
240 Wang, X., Bahri, M., Fu, Z. et al. (2021). *J. Am. Chem. Soc.* 143: 15011–15016.
241 Yue, Y., Cai, P., Xu, K. et al. (2021). *J. Am. Chem. Soc.* 143: 18052–18060.
242 Yang, X., Gong, L., Wang, K. et al. (2022). *Adv. Mater.* 34: 2207245.
243 Sharma, A., Eadi, S.B., Noothalapati, H. et al. (2024). *Chem. Soc. Rev.* 53: 2530–2577.
244 Meng, Z., Aykanat, A., and Mirica, K.A. (2019). *J. Am. Chem. Soc.* 141: 2046–2053.

245 Aykanat, A., Meng, Z., Stolz, R.M. et al. (2022). *Angew. Chem., Int. Ed.* 61: e202113665.
246 Wang, M., Zhang, Z., Zhong, H. et al. (2021). *Angew. Chem., Int. Ed.* 60: 18666–18672.
247 Liu, Q., Sun, Q., Shen, J. et al. (2023). *Coord. Chem. Rev.* 482: 215078.
248 Liu, W., Pan, H., Liu, C. et al. (2019). *ACS Appl. Mater. Interfaces* 11: 11466–11473.
249 Zhang, J., Zhang, J., He, F. et al. (2021). *Nano-Micro Lett.* 13: 1–30.
250 Bai, S. and Shen, X. (2012). *RSC Adv.* 2: 64–98.
251 Maiti, U.N., Lee, W.J., Lee, J.M. et al. (2014). *Adv. Mater.* 26: 40–67.
252 Chen, G., Wan, H., Ma, W. et al. (2020). *Adv. Energy Mater.* 10: 1902535.
253 Liu, W., Wang, C., Zhang, L. et al. (2019). *J. Mater. Chem. A* 7: 3112–3119.
254 Yang, S.X., Yu, Y.H., Dou, M.L. et al. (2020). *J. Am. Chem. Soc.* 142: 17524–17530.
255 Han, N., Wang, Y., Ma, L. et al. (2017). *Chem* 3: 652–664.
256 Ji, W., Wang, T.-X., Ding, X. et al. (2021). *Coord. Chem. Rev.* 439: 213875.
257 Ding, X. and Han, B.H. (2015). *Angew. Chem. Int. Ed.* 54: 6536–6539.
258 Ding, X. and Han, B.-H. (2015). *Chem. Commun.* 51: 12783–12786.
259 He, W.-L. and Wu, C.-D. (2018). *Appl. Catal. B-Environ.* 234: 290–295.
260 Roy, S. and Reisner, E. (2019). *Angew. Chem., Int. Ed* 58: 12180–12184.
261 Chen, J., Zou, K., Ding, P. et al. (2019). *Adv. Mater.* 31: 1805484.
262 Yang, X.Y., Jin, Y.C., Yu, B.Q. et al. (2022). *Sci. China Chem.* 65: 1291–1298.